Imperial College London

MSc Quantum Fields and Fundamental Forces

Generation of a Primordial Gravitational Wave Background during Inflation

22nd September 2022

Author:
Nur Imanina Binti
Mohd Faidzal
CID: 01492374

Supervisor:
Dr. Carlo Contaldi
Theory Group
Department of Physics

Abstract

Primordial gravitational waves are essential in probing the initial conditions of the early universe. This dissertation is a self-contained review of primordial gravitational waves generated during inflation, an evolutionary epoch in which cosmological scales of the universe underwent a rapid, accelerated expansion driven by negative pressure. By restricting to a flat, homogeneous and expanding universe described by the Friedmann-Robertson-Walker metric, it addresses the inconsistencies of cosmological observation with regards to the successful hot Big Bang model. Thus, a brief overview of inflation is provided with emphasis on the single-field slow-roll approximation model. Within this framework, primordial perturbations are considered by introducing a tiny perturbative expansion to the metric up to linear order. Using the perturbed metric, the perturbed Einstein equations are derived in great detail to determine the evolution of scalar and tensor perturbations during inflation as well as their physical interpretation. Transitioning from theory to observation, these perturbations are quantised to determine their power spectra and the spectral indices that characterise them. From these, the consistency condition for a single-field slow-roll inflationary model is formulated. A brief explanation on their significance with respect to probing inflation as well as their relation to primordial gravitational wave-detection is given. Finally, some old and recent development in primordial gravitational wave-detection are discussed.

Contents

Acknowledgements

Firstly, I would like to thank my supervisor, Dr. Carlo Contaldi on his guidance, feedback and our enlightening discussions throughout the dissertation period. When I first came to him in June, I was hoping to work on gravitational waves and their observations, and he offered me a new perspective by introducing me to *primordial gravitational waves*. As I started my background reading surrounding these exotic objects, it gave me newfound excitement and I am very thankful to have completed my dissertation on my chosen topic.

Next, many thanks to Carlos Barredo, Andrew King, Paul Krüper and Sam Bysh, my friends from the QFFF cohort for their continuous support and fruitful discussions throughout the examination and dissertation months, and for their willingness to proofread my written work.

Last but not least, I would like to express my utmost love and gratitude for my family and close friends who were always there for me through my ups and downs this past year. My undertaking of the QFFF programme was one of the most trying times of my life, but they made it bearable with their endless support and readiness to lend an ear whenever I needed it. It is because of them, that I am able to believe in myself.

I will forever cherish the knowledge and lessons learned from this experience.

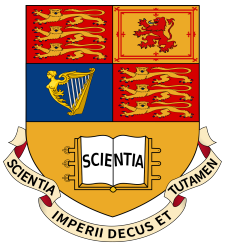

1 Introduction

This section provides background context to the topic of dissertation.

1.1 Gravitational Waves as a Cosmological Probe

1.1.1 A Brief History of General Relativity

It is a historical fact that Einstein's theory of general relativity (published in 1916) garnered widespread interest from both the scientific community and general public - common folk marvelled at the man who held so much knowledge of the universe while his peers offered their own interpretation and further study of his work [26]. Developed as an extension to his theory of special relativity (which was published a decade prior), general relativity introduced to physicists, the notion of gravity as a curvature in spacetime - a jarring exposition to the long-standing Newtonian establishment - as well as the likes of tensor calculus. Nonetheless, the prospects of this theory were promising; by utilising the equivalence principle (also formulated by Einstein), it is shown that general relativity is perfectly consistent with special relativity, where Newtonian equations hold. Furthermore, the theory has contributed greatly to our understanding of the universe by predicting natural occurrences and objects whose lack of observation was due to technological shortcomings of its time and by clarifying the nuances in observation that were formerly unexplained.

In a separate publication in 1915, Einstein confirmed that the precession rate of Mercury about the Sun predicted by his ground-breaking theory accounted for the discrepancy measured by astronomers [68]. The same result was unattainable in the case of a Newtonian potential, thus solidifying general relativity as a general theory of gravity[1]. Later in 1919, Arthur Eddington and Frank Dyson sought to prove the crux of Einstein's theory of general relativity in two-pronged experiments that involved measuring the positions of the Hyades - a bright cluster of stars - during a total solar eclipse and at night, in the absence of the sun and the moon [40]. Their findings concluded a light deflection of 1.61 arcseconds during the eclipse, thus supporting Einstein's prediction that light bends in the presence of a massive object [24]. The study was not free of controversy - there were doubts concerning the legitimacy of Eddington's data, which had no concrete resolve as his original photographic plates where the measurements were taken were permanently lost [22]. Regardless, these experiments granted Einstein global celebrity status; the story of two English astronomers proving the postulates of a German theorist in the wake of the war was riveting [40].

1.1.2 The Search for Gravitational Waves

By the end of the 20^{th} century, gravitational waves (GWs) were the last prediction of general relativity left undiscovered[2]. By considering a small deviation on a flat metric and its energy-momentum tensor, Einstein eventually arrived at a description of transverse waves with two distinct polarisations travelling at the speed of light. Based on his calculations, these ripples in spacetime would require an aggressively fast-moving or fast-rotating source to reach Earth with detectable amplitudes. Despite their elusive nature, scientists were determined in their quest for GWs after a study in 1981 confirmed that the increasing rotation of the binary neutron star system, PSR B1913+16 was consistent with its predicted GW-emission [70]. Finally, in 2015, detectors of the Laser Interferometer Gravitational-wave Observatory (LIGO) observed

[1] While Einstein has tried to reproduce his calculations for other planets, the results did not match [68].

[2] The first image of a black hole was produced in 2019 [6], but its first evidence came in the form of X-ray emission from Cygnus X-1 in 1964 [49].

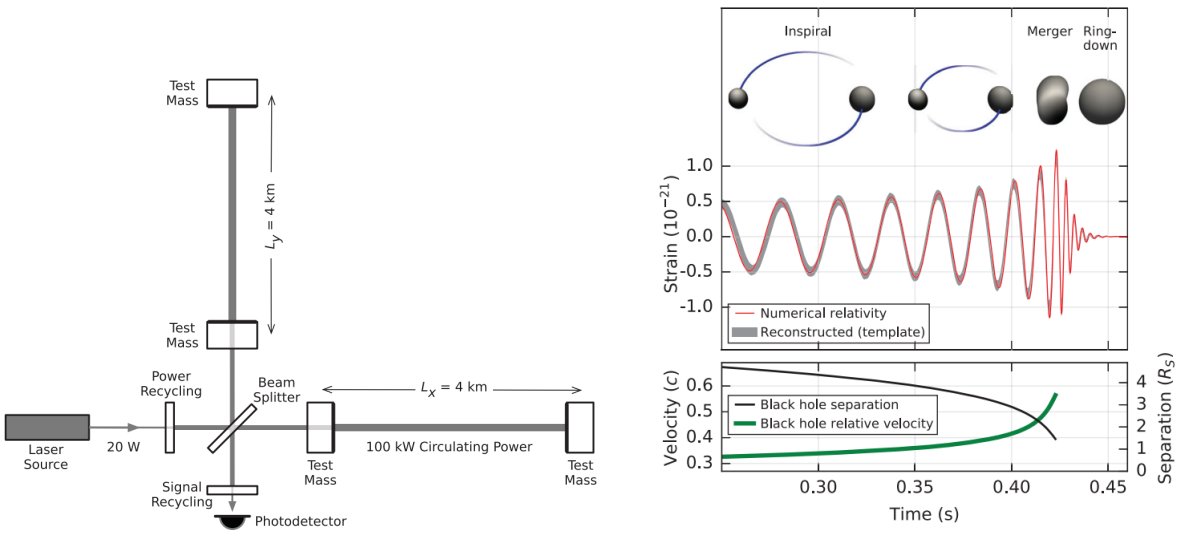

Figure 1: The image on the left shows a simple schematic (not to scale) of an Advanced LIGO (aLIGO) detector used during the detection, whose mechanisms are based off the Michelson interferometer. The image on the right compares the ringdown of the two black holes with their corresponding separation, velocity and gravitational wave emission. The peak strain, 1.0×10^{-21} was emitted at the point of merger. Both images were taken from [1].

signals of GWs emitted by a binary black hole merger - marking the first direct evidence of GWs since their prediction a century prior [1]. Basing their design (Figure 1) on the Michelson interferometer from the infamous Michelson-Morley experiment, LIGO's highly sensitive interferometer was able to detect the full frequency range of these signals (30Hz to 250Hz), with a peak GW-strain of 1.0×10^{-21} [1], seen in Figure 1. The LIGO detection was exciting because it symbolised a plethora of possibilities beyond. Since the physical establishment of GWs, there is much hope in using them as probes - the way visible and infrared light have been used in astronomy - to tell us more about the universe, with various proposals to improve current detectors and develop new ones to support them.

Of particular interest to cosmologists is their use in probing the initial conditions of the early universe. Following observations which were deemed inconsistent with the successful hot Big Bang model, the theory of inflation was introduced to address these anomalies [7, 30, 44]. However, it was also immediately recognised as a fitting mechanism to explain the origins of primordial perturbations in the universe [13, 31, 32, 64]. The inflationary epoch is described as a period in which the scale factor (a parameter characterising the expansion of the universe) undergoes a rapid, accelerated expansion driven by negative pressure due to a plausible scalar field also named as 'inflation' [43]. In theory, the inhomogeneous matter distribution had induced quantum fluctuations about the metric which are later stretched to cosmic scales [58]. These acted as seeds of the large-scale structure of our universe. Among the perturbed Einstein equations, the ones due to the tensor perturbations result in wave equations with their solutions corresponding to GWs [23]. Unlike the GWs observed by LIGO, these *primordial gravitational waves* (PGWs) are products of the inhomogeneities of the early universe. Their existence requires no matter source. By building upon past and current work on GW-detection and fine-tuning to the primordial case, the goal is to use these observations to gain insight on the details of inflation.

1.1.3 Dissertation Objectives

This dissertation aims to:

1. Understand the origins of primordial perturbations in the universe.

2. Link their theoretical framework to research and observations of PGWs.

To achieve the first objective, an overview of the theory of inflation[3] is provided in the proceeding subsection. Then, the primordial perturbations generated in this framework will be introduced in Section 2. The two subsequent sections following this will focus on the mathematical aspects of the perturbations. In Section 3, the Einstein equations perturbed by the primordial perturbations are derived in full detail under the guide of [23], to provide insight to their physical interpretation. The second objective is achieved in Sections 4 and 5. In the former, calculations of the primordial perturbation power spectra and their related quantities are demonstrated, closely following the working presented in [69], whereas the latter summarises some recent development on PGW-detection. Lastly, a final conclusion will be given in Section 6.

[3]The only cosmological theory that successfully accounts for these perturbations.

1.2 The Theory of Inflation

1.2.1 The Expanding Universe

The main goal of modern cosmology is to develop a theoretical framework of how the universe came to be which is consistent with observational data leading up to today. The hot Big Bang model is taken as the standard model of cosmology. The term *big-bang* was first coined in 1948, though the theory it encapsulated back then was very different to the one we associate it with today [67]. Based on the cosmological principle that assumes homogeneity and isotropy of the universe at large scales, the new and improved hot Big Bang model describes an extremely hot and dense universe that cools as it expands over time with its expansion characterised by the scale factor, $a(t)$. The variation of $a(t)$ over cosmic time, t depends on the type of energy driving the expansion[4]. Thus, the universe began approximately 13.8 billion years ago, with a singularity from which space expanded through three successive epochs classified by their dominating energies; radiation, matter and dark energy[5] [23]. In relation to this, the Hubble rate, H is a useful parameter in quantifying the variation of the scale factor with respect to energy,

$$H(t) \equiv \frac{\dot{a}}{a}, \tag{1.1}$$

where $\dot{a} \equiv \frac{da}{dt}$. To determine the Hubble rate for each epoch, one can substitute in the relation between the scale factor and cosmic time, $a \propto t^{1/2}$, $a \propto t^{2/3}$, $a \propto \exp(H_0 t)$ for the radiation-dominated, matter-dominated and dark-energy-dominated epochs respectively.

The concept of an expanding universe is also consistent with general relativity as its origins are traced back to early attempts at establishing a relativistic cosmological model. Built on the foundation of Einstein's static solution, Aleksandr Friedmann and Georges Lemaître were the first few to independently derive a non-static model of a universe undergoing a cosmic expansion [27, 41]. By adopting the signature $(-+++)$, in general relativity, a flat, expanding universe is described by the Friedmann-Robertson-Walker (FRW) metric,

$$g_{\mu\nu} = \begin{pmatrix} -1 & 0 & 0 & 0 \\ 0 & a^2(t) & 0 & 0 \\ 0 & 0 & a^2(t) & 0 \\ 0 & 0 & 0 & a^2(t) \end{pmatrix}, \tag{1.2}$$

which is used to form the spacetime interval,

$$\mathrm{ds}^2 = -\mathrm{dt}^2 + \mathrm{a}^2(\mathrm{t})\mathrm{dx}^\mathrm{i}\mathrm{dx}^\mathrm{j}. \tag{1.3}$$

An equivalent spacetime interval in terms of conformal time, η is

$$\mathrm{ds}^2 = \mathrm{a}^2(\eta)(-\mathrm{d}\eta^2 + \mathrm{dx}^\mathrm{i}\mathrm{dx}^\mathrm{j}). \tag{1.4}$$

One can derive the latter expression from the former, via the relation between conformal time and cosmic time,

$$\eta \equiv \int_0^\mathrm{t} \frac{1}{\mathrm{a}(\mathrm{t}')}\,\mathrm{dt}'. \tag{1.5}$$

Note that in this relation, the apostrophes are used to distinguish t in the integrand and as an upper limit of the integration. By applying this metric in the Einstein Field Equations (EFE), one would arrive at the Friedmann equations - a set of two dynamical equations governing this cosmological model.

[4] Expansion of space between two distances.

[5] Following the observation of 10 accelerating Type Ia supernovae [59], it is likely that the universe is currently in the dark energy-dominated epoch.

The first step in deriving the Friedmann equations is to consider the EFE, which are a set of equations relating the geometry of spacetime (left-hand side or LHS) to its matter distribution (right-hand side or RHS),

$$G^{\mu}_{\nu} \equiv g^{\mu\gamma}\left[R_{\gamma\nu} - \frac{1}{2}g_{\gamma\nu}\mathcal{R}\right] = \frac{8\pi G_N}{c}T^{\mu}_{\nu}, \tag{1.6}$$

where G^{μ}_{ν} is the Einstein tensor expressed as a combination of the Ricci tensor, $R_{\gamma\nu}$ and Ricci scalar, $\mathcal{R}$ contracted by the inverse perturbed FRW metric, $g^{\gamma\nu}$. $G_N = 6.67 \times 10^{-11}\text{Nm}^2\text{kg}^{-2}$ is Newton's gravitational constant, c is the speed of light and T^{μ}_{ν} is the energy-momentum tensor (EMT). To derive the EFE, one needs to determine $R_{\gamma\nu}$, $\mathcal{R}$ and T^{μ}_{ν}. Recall that the Ricci tensor and Ricci scalar are defined as

$$R_{\gamma\nu} = \Gamma^{\alpha}_{\gamma\nu,\alpha} - \Gamma^{\alpha}_{\gamma\alpha,\nu} + \Gamma^{\alpha}_{\beta\alpha}\Gamma^{\beta}_{\gamma\nu} - \Gamma^{\alpha}_{\beta\nu}\Gamma^{\beta}_{\gamma\alpha} \tag{1.7}$$

and

$$\mathcal{R} = g^{\gamma\nu}R_{\gamma\nu} \tag{1.8}$$

respectively. In equation (1.7), $\Gamma^{\alpha}_{\mu\nu}$ is the Christoffel symbol, expressed as

$$\Gamma^{\alpha}_{\mu\nu} = \frac{1}{2}g^{\alpha\gamma}(g_{\gamma\mu,\nu} + g_{\gamma\nu,\mu} - g_{\mu\nu,\gamma}), \tag{1.9}$$

where we swapped the dummy indices γ and μ. Thus, in equation (1.7), $\Gamma^{\alpha}_{\mu\nu,\alpha}$ is the Christoffel symbol's derivative with respect to α. The temporal part ($\mu = \nu = 0$) of equation (1.6) forms the first Friedmann equation whereas the second Friedmann equation is the combination of this temporal part and its spatial counterpart ($\mu = i, \nu = j$)[6]. Before proceeding with the derivation, it is useful to determine the inverse FRW metric,

$$g^{\mu\nu} = \frac{1}{a^2(t)}\begin{pmatrix} -a^2(t) & 0 & 0 & 0 \\ 0 & 1 & 0 & 0 \\ 0 & 0 & 1 & 0 \\ 0 & 0 & 0 & 1 \end{pmatrix}. \tag{1.10}$$

To determine all the non-zero Christoffel symbols, the following cases for both $\alpha = 0$ and $\alpha = k$ must be considered:

1. $\mu = \nu = 0$
2. $\mu = 0, \nu = i$
3. $\mu = i, \nu = j$.

One would find that the only non-zero Christoffel symbols are

$$\Gamma^{0}_{ij} = \delta_{ij}\dot{a}a \;\text{ and }\; \Gamma^{i}_{0j} = \Gamma^{i}_{j0} = \delta_{ij}\frac{\dot{a}}{a}. \tag{1.11}$$

Using these values, one can proceed to find the temporal and spatial Ricci tensors,

$$\begin{aligned} R_{00} &= -3\frac{\ddot{a}}{a}, \\ R_{ij} &= g_{ij}\left(\frac{\ddot{a}}{a} + 2H^2\right), \end{aligned} \tag{1.12}$$

[6]The derivation steps used in this dissertation closely resembles that in [61] but modified for the FRW metric.

where H here is the Hubble rate defined in equation (1.1). By contracting these with their respective FRW metric components, g_{00} and g_{ij}, we obtain the Ricci scalar,

$$\begin{aligned}\mathcal{R} &= -R_{00} + \frac{1}{a^2}R_{ii} \\ &= 6\left[\frac{\ddot{a}}{a} + \left(\frac{\dot{a}}{a}\right)^2\right] \\ &= 6\left(\frac{\ddot{a}}{a} + H^2\right),\end{aligned} \tag{1.13}$$

where R_{ii} comes from eliminating the delta function in $g_{ij} = \delta_{ij}\frac{1}{a^2(t)}$ by setting $j = i$. Lastly, one needs to consider the temporal and spatial parts of the energy-momentum tensor, T^{μ}_{ν}. In general, T^0_0 is just the energy density, ρ whereas $T^i_j = \delta^i_j P$, which is the pressure pointing in each spatial direction. With this last step, one has all the ingredients to compute the Friedmann equations which are summarised as:

$$\left(\frac{\dot{a}}{a}\right)^2 = \frac{8\pi\rho}{3}, \tag{1.14}$$

$$\frac{\ddot{a}}{a} = -\frac{4\pi}{3}(\rho + 3P). \tag{1.15}$$

Equation (1.14) is the first Friedmann equation and equation (1.15) is the second Friedmann equation.

Here, the constants G_N and c are set to 1. The smooth, expanding universe framework is widely accepted as it coincides with observational data such as the Cosmic Microwave Background (CMB) - expected remnants of the Big Bang in the form of blackbody radiation with a temperature of $T = 2.728$K [50] - and the measurement of receding velocities of nearby observable galaxies, which led to the formulation of Hubble's law [37]. It also provides a detailed collection of the Big Bang nucleosynthesis which matches the matter composition of the universe today [65]. Despite the successes of the Hot Big Bang model, there are some subtleties to be considered.

1.2.2 The Horizon Problem

One of the nuances related to this model is the *Horizon/Homogeneity Problem*; it concerns the causal relationship[7] between particles in our universe. Two quantities crucial in the discussion of this problem are the *comoving horizon*[8], η and the *comoving Hubble radius*, $\frac{1}{a(t)H(a)}$. The relation between them is derived by considering equation (1.1) in the definition (1.5):

$$\eta \equiv \int_0^{\mathrm{a}} \frac{1}{\mathrm{a}'} \frac{1}{\mathrm{a}'\mathrm{H}(\mathrm{a}')} \, \mathrm{da}', \tag{1.16}$$

where the apostrophes are used in a similar fashion to (1.5).

By physical interpretation, η is the "maximum comoving distance travelled by light since the beginning of the universe" whereas $\frac{1}{aH}$[9] is the "distance over which particles can travel in the course of one expansion time" [23]. Thus, particles separated by η and $\frac{1}{aH}$ are not causally-connected. The only subtle difference is, this condition is fixed for η (nothing is faster than the speed of light, thus no information can travel beyond this distance), but changeable for $\frac{1}{aH}$ [23], as H is a-dependent. In the context of observations, η corresponds to the furthest distance from which light signals can reach us [63]. CMB observations show that the universe is homogeneous and isotropic on all scales since the time of recombination[10] until today [47]. As light from regions on opposite directions to Earth would take the same amount of time to reach us (equivalent to the time period since the Big Bang), it is impossible for these regions to have interacted with one another [63]. This raises the question, *how could non-interacting*[11] *regions achieve uniform temperature and appear homogeneous?*

A plausible suggestion is that at early times, $\frac{1}{aH}$ was much larger than η, hence the disconnected regions observed today were actually causally-connected then. Thus, to achieve the configuration today where η exceeds $\frac{1}{aH}$, the comoving Hubble radius would have had to undergo a period in which it decreased with time. Recalling the relation between the scale factor and cosmic time, this period could not have occurred during any of the three aforementioned epochs in the standard model of the universe, as the expansion characterised by $a(t)$ throughout these epochs would mean that $\frac{1}{aH}$ increases with time. The only possible scenario is that there must be an intermediate evolutionary process between the point of singularity and the radiation dominated epoch in which the size of the comoving Hubble radius decreased. In response to this, in 1981, Alan Guth proposed the theory of *inflation*, a time period preceding the radiation-dominated epoch, in which the scale factor, $a(t)$ undergoes a rapid, accelerated expansion.

[7] Two events are causally-connected if one affects the other and their causal order is preserved.

[8] Also known as *conformal time*, as introduced in (1.4). Another term for η is *particle horizon*.

[9] The implicit dependence of a on t and H on a is assumed henceforth.

[10] Recombination refers to the period succeeding nucleosynthesis in which radiation temperatures are well below the ionisation energy of atoms thus allowing ions and electrons to form neutral hydrogen atoms [71].

[11] In other words, *not causally-connected*.

1.2.3 Inflation: An Overview

The theory of inflation is best understood by looking at its stages independently; pre-inflation, during inflation, end of inflation and post-inflation, with references to Figure 2.

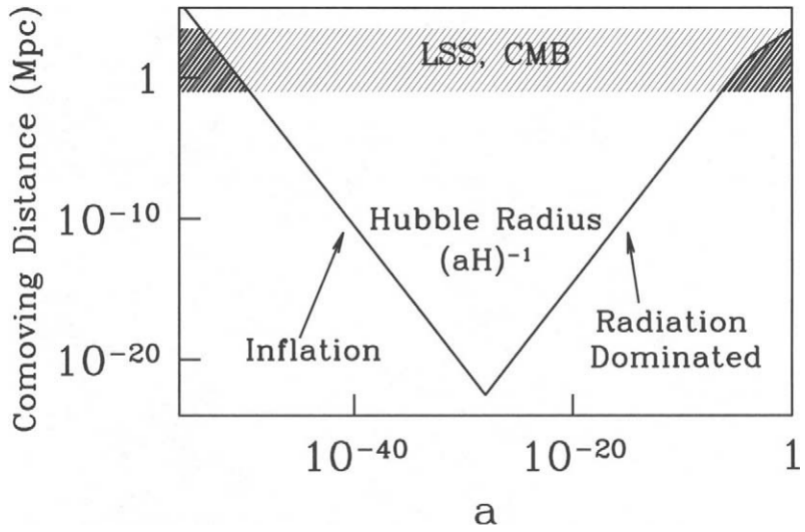

Figure 2: A visual aid in understanding the evolution of the universe from the inflationary epoch into the radiation and matter-dominated epochs taken from *Modern Cosmology* by Dodelson, 2003 [23]. *Comoving distance* here is synonym to the comoving Hubble radius, $\frac{1}{aH}$. It decreases during the inflation period until it stops and increases, signifying the end of inflation and the start of the radiation-dominated epoch. Furthermore, the point at which the slope of the graph declines is when the matter-dominated epoch has started, indicating a decelerating expansion of the universe. The shaded band represents scales of cosmological interests, with the darker shades indicating the scales to be within the Hubble radius and the lighter shades, beyond it.

Pre-Inflation While this period is not shown in Figure 2, it is assumed to have taken place in the very early age of the universe, when all scales of cosmological interests were smaller than the comoving Hubble radius. Therefore, these scales were causally-connected, thus would have been able to interact and eventually reach homogeneity during this time.

During Inflation Inflation was suggested as the epoch in which the comoving Hubble radius, $\frac{1}{aH}$ decreased in time, taking place about 10^{-36} seconds into the expansion of the singularity. For this to happen, aH must increase in time, $aH > 0$. By considering this evolution, it is found that the scale factor, $a(t)$ must have undergone an accelerated expansion,

$$\frac{d}{dt}\left[a\frac{\dot{a}}{a}\right] = \ddot{a} > 0,$$

leading to the definition of *inflation* proposed previously in subsubsection 1.1.2. To better understand the magnitude of this accelerated expansion, consider the energy scale of 10^{15}GeV, which is taken as the minimum threshold for inflation to occur in most inflationary models [23]. If the universe had remained in the radiation-dominated epoch since the end of inflation, H would have scaled as a^{-2}, hence $\frac{a_0 H_0}{a_e H_e} = {a_e}^{12}$ [23]. If the temperature during a_e is 10^{15}GeV, then the scale factor at the end of inflation would have been $a_e \simeq T_0/10^{15}\text{GeV} \simeq 10^{-28}a_0$. As the comoving Hubble radius at the start of inflation must be much larger than its size today, it would have had to shrink by at least 28 orders of magnitude [23]. By solving the differential

[12]The subscript 0 refers to values of today whereas the subscript e refers to values at the end of inflation.

equation $da/a = Hdt$ in which we assume a constant H, the expansion is described by the following exponential equation:

$$a(t) = a_e \exp H(t - t_e), \tag{1.17}$$

where $t < t_e$. Hence, for a to have increased by 10^{28} during inflation, we require a minimum argument of $H(t - t_e) \approx 64$ for the exponential[13]. Whilst undergoing this rapid expansion, the homogeneity achieved among scales within the Hubble radius, $\frac{1}{aH}$ pre-inflation is preserved regardless of the conditions of scales beyond this homogeneous region [47]. Hence, inflation solves the horizon/homogeneity problem[14]. In the following subsubsections, we will look at the driving force behind this expansion and the slow-roll approximation model of inflation.

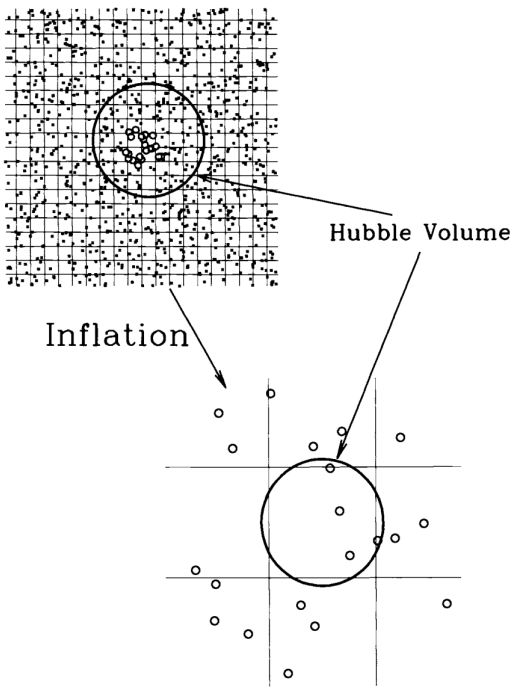

Figure 3: An intuitive depiction of the accelerated expansion undergone by the scale factor, a during inflation (not to scale) taken from *Modern Cosmology* by Dodelson, 2003 [23]. The grids represent the measurement of a whereas the circles are the comoving Hubble radius, $\frac{1}{aH}$ before and after inflation. Where it held multiple grids pre-inflation, it barely holds one grid post-inflation.

End of Inflation At the end of inflation, the comoving horizon, η greatly exceeds the Hubble radius, $\frac{1}{aH}$, as roughly depicted in Figure 3. It is with this relative size between the two that the universe transitions into the radiation, matter and dark energy-dominated epochs. Hence, the homogeneous and isotropic CMB observations are explained.

Post-Inflation As seen in Figure 2, after the inflationary epoch ends, the Hubble radius begins to expand, as per the scale factor-cosmic time relation for each epoch. In the same figure, the scales of cosmological interest (shaded band) re-enters the horizon around the time of the matter-dominated epoch. Since it took about 60 e-folds to achieve this, we can infer that the scales which have entered the horizon today are similar to the ones that left it at the start of inflation [23]. Therefore, much ongoing work aims to extract information about the early stage of the universe from today's measurement of the CMB, especially those related to the initial conditions of inflation and the primordial perturbations that have contributed to the large-scale structure of the universe.

[13]Note that different sources vary in the argument's exact value. For example, in Mukhanov's *Physical Foundations of Cosmology*, this value is at least 75 [47].

[14]Apart from the horizon/homogeneity problem, inflation also solves other nuances such as the flatness problem, the monopole problem and the origin of the large-scale structure problem [65].

1.2.4 The Driving Force of Inflation

The first step in determining the source of the inflationary epoch is to identify the energy driving its expansion. By recalling the second Friedmann equation, (1.15) and noting that d^2a/dt^2 is positive during inflation, we require an overall minus sign on the RHS of the equation and thus, $-\rho - 3P < 0$. After rearranging the terms, we arrive at the following relation:

$$P < -\frac{\rho}{3}.$$

However, since it is impossible for energy densities to be negative, this means that inflation must be driven by a form of energy with negative pressure, instead. The only known energy with negative pressure thus far is dark energy, whose links to the early universe was investigated in 2007 by the Higher-Z Supernova Search Team, which was led by Adam Riess of the Johns Hopkins University [62]. By observing Type Ia supernovae at very high redshifts, their findings indicated that dark energy has existed for at least 10 billion years [62], although there was no hint regarding its candidacy as a driving force of inflation. Since then, more studies have been done on the explicit link between dark energy and inflation [11, 66], however this is beyond the scope of the dissertation.

Guided by this establishment, various guesses were made regarding the source of inflation along with the development of their corresponding models. However, the discussion in determining the most accurate inflationary model[15] is inconclusive due to lack of observational evidence to favour either of them [36]. Thus, the true source of inflation is still unknown to this day. Nonetheless, these models act as useful guides in understanding the details of inflation as well as predicting plausible observations. This dissertation considers the simplest among these models - one that assumes a generic scalar field, φ called 'inflation' to be the only matter field existing during the early stages of the universe [66]. This scalar field would possess the negative pressure driving the inflationary expansion. Note that φ is unrelated to any known physics to date, as constraints on scalar fields in the Standard Model have ruled them out as possible candidates. The scalar field is generally inhomogeneous, $\varphi(t, \vec{x}) = \varphi^{(0)}(t) + \delta\varphi(t, \vec{x})$[16], but we will only consider its homogeneous part, $\varphi^{(0)}$ in this section. Its action is written as [42]:

$$\mathcal{S} = -\int \sqrt{-g}\left[\frac{1}{2}\partial_\mu\varphi\partial^\mu\varphi + V(\varphi)\right] \mathrm{d}^4\mathrm{x}. \tag{1.18}$$

We can derive its energy density and pressure equations by considering its energy-momentum tensor,

$$T^{\alpha(0)}_\beta = -g^\alpha_0 g^0_\beta(\dot{\varphi}^{(0)})^2 + g^\alpha_\beta\left[\frac{1}{2}(\dot{\varphi}^{(0)})^2 - V(\varphi^{(0)})\right],$$

where only the time-dependence of φ is relevant. The temporal and spatial components lead to the energy density and pressure of $\varphi^{(0)}$ respectively:

$$\begin{aligned} \rho &= \frac{1}{2}(\dot{\varphi}^{(0)})^2 + V(\varphi^{(0)}), \\ P &= \frac{1}{2}(\dot{\varphi}^{(0)})^2 - V(\varphi^{(0)}). \end{aligned} \tag{1.19}$$

By examining the pressure equation in (1.19), it is inferred that φ would possess negative energy under the condition that its potential energy surpasses its kinetic energy, $V(\varphi) >> \frac{\dot{\varphi}}{2}$.

[15] To understand the difference between an inflationary *model* and an inflationary *scenario*, refer to subsection 1.3.

[16] The time and spatial dependence of φ is understood henceforth. Their expressions will be neglected to avoid cluttering.

1.2.5 The Slow-Roll Approximation Model

The first suggestion by Guth in accordance with this condition, the model in which φ is suspended in a false vacuum (a local minimum of its potential) for at least 60 e-folds before it reaches the true vacuum (the global minimum of its potential), was unfeasible as calculations showed the latter state would never be achieved [33, 35]. In response to this, the slow-roll approximation model was proposed. It entails φ slowly rolling towards the true ground state such that it never reaches its destination within the time period of interest.

To determine the evolution equation of φ in this model, we substitute its energy density, ρ (which in this case, is close to a constant) into the first Friedmann equation and differentiate it with respect to cosmic time, t. This gives

$$2\frac{\dot{a}}{a}\left[\frac{\ddot{a}}{a} - H^2\right] = \frac{8\pi G_N}{3}[\dot{\varphi}^{(0)}\ddot{\varphi}^{(0)} + V_\varphi \dot{\varphi}^{(0)}], \tag{1.20}$$

where $V_\varphi = \frac{dV}{d\varphi^{(0)}}$. By substituting the first and second Friedmann equations, the LHS becomes

$$-8\pi G_N H(\rho + P) = -8\pi G_N H(\dot{\varphi}^{(0)})^2.$$

Equating this with the RHS of equation (1.20) leads to the following evolution equation of inflation, the scalar field,

$$\ddot{\varphi}^{(0)} + 3H\dot{\varphi}^{(0)} + V_\varphi = 0, \tag{1.21}$$

whose equivalent expression using conformal time, η is

$$\varphi''^{(0)} + 2aH\varphi'^{(0)} + a^2 V_\varphi = 0. \tag{1.22}$$

A notable consequence of φ slowly rolling is that the Hubble rate also changes slowly such that it is often taken as a constant in calculations. With such an assumption, the conformal time becomes

$$\eta \equiv \frac{1}{H}\int_{\mathrm{a_e}}^{\mathrm{a}} \frac{1}{\mathrm{a'^2}}\,\mathrm{da'} \approx -\frac{1}{\mathrm{aH}},$$

where again, the apostrophe is used to distinguish between the scale factor in the limits of integration and in the integrand. Here, a is the scale factor during inflation whereas a_e is the scale factor at the end of inflation. Since $a_e >> a$ due to the exponential expansion, the overall term bears a minus sign.

Furthermore, there are two parameters which are used to specifically quantify the slow roll. They are

$$\epsilon = -\frac{\mathrm{d\,ln\,H}}{\mathrm{d\,ln\,a}} \equiv -\frac{\dot{H}}{H^2} \tag{1.23}$$

and

$$\tau = \frac{\mathrm{d\,ln}\,\epsilon}{\mathrm{d\,ln\,a}} \equiv \frac{\dot{\epsilon}H}{\epsilon}. \tag{1.24}$$

In this model, these variables are extremely small ($<< 1$) and in the limit where φ is constant, they vanish. We will revisit these parameters in Section 4 in our derivation of the power spectra related to inflation, and in our consideration of how measuring these parameters may hint at the physics of inflation. This subsubsection marks the end of the preliminary knowledge required to proceed with the crux of the dissertation - the primordial perturbations generated during inflation. We begin our voyage on this topic by considering linear perturbations to the metric in Section 2. Then, subsequent sections will cover some calculations related to these metric perturbations.

1.3 Definitions and Notations

We end the introductory section with a compilation of all the scientific definitions and notations used throughout the dissertation. While they are uniquely introduced at different stages of the dissertation, this list acts as a reference, mid-reading. The definitions are arranged in alphabetical order with their notations (if applicable) and page numbers (where first mentioned) alongside.

Notation	Definition	Page
$\mathcal{H}_{ij}$	**A divergenceless traceless symmetric tensor** that characterises the tensor perturbations to the FRW metric which are linked to PGWs.	21
Θ	**Anisotropies** generated by tensor perturbations from $\mathcal{H}_{ij}$.	41
$\hat{a}^{\dagger}_{\vec{k}}$	**Annihilation operator:** an operator that lowers the number of particles/energy of a quantum-mechanical system	46
N/A	**Baryogenesis:** the process responsible for the excess of baryonic matter over baryonic antimatter in the universe.	19
N/A	**Blue-tilted spectrum:** a term used to describe when the observed spectral indices exceed unity	51
$\Gamma^{\alpha}_{\mu\nu}$	**Christoffel symbol:** a rank-3 tensor that dictates the transformation of a law in the local intertial frame (LIF) as seen by an external observer.	8
$\frac{1}{aH}$	**Comoving Hubble radius:** the distance over which particles can travel in the course of one expansion time.	10
$\mathfrak{R}$	**Comoving curvature perturbation:**	47
N/A	**Conformal Newtonian gauge:** a gauge choice in which the scalar functions $B = E = 0$ thus leading to $\phi = \Phi$ and $\psi = \Psi$.	21
η	**Conformal time (Comoving horizon):** the maximum comoving distance travelled by light since the beginning of the universe.	7
$r \approx -8n_t$	**Consistency condition** for a single-field slow-roll model of inflation.	49
N/A	**Cosmic Microwave Background (CMB):** remnants of the Big Bang in the form of blackbody radiation with a temperature of $T = 2.728$K.	9
t	**Cosmic time (Cosmological time):** a time coordinate used in the Big Bang models of physical cosmology.	7
N/A	**Cosmological principle:** The assumption that the universe is homogeneous and isotropic at large scales.	7
$\hat{a}_{\vec{k}}$	**Creation operator:** an operator that raises the number of particles/energy of a quantum-mechanical system	46
N/A	**Dark-energy dominated epoch:** A cosmological epoch in which dark energy dominates and causes an accelerated expansion in which the scale factor varies as $a \propto \exp(H_0 t)$.	7
N/A	**Decomposition theorem:** a theorem that states the three different types of metric perturbations are independent of one another [23].	22
S_i F_i	**Divergenceless vectors** that characterises the vector perturbations about the FRW metric which decay very fast.	20
G^{μ}_{ν}	**Einstein Tensor:** a rank-2 tensor used to describe spacetime curvature.	8
N/A	**Einstein field equations:** a set of equations relating the geometry of spacetime to its matter distribution.	7

Notation	Definition	Page
ρ	**Energy density:** the amount of energy stored in an arbitrary system or region of space per unit volume.	9
T^{μ}_{ν}	**Energy-momentum tensor:** a rank-2 tensor that describes the density and flux of energy and momentum in spacetime.	8
H_k	**Expression** of $H = \frac{k}{a}$ at horizon crossing.	45
N/A	**Friedmann equations:** a set of two dynamical equations governing the hot Big Bang cosmological model.	7
$g_{\mu\nu}$	**Friedmann-Robertson-Walker (FRW) metric:** the metric which describes a flat and expanding universe.	7
∇	**Gradient operator:** an operator that calculates the gradient of a differentiable multi-variable scalar function f.	45
N/A	**Gravitational waves (GWs):** transverse waves with two polarisations travelling at the speed of light propagating through a gravitational field which are produced by a moving or disturbed source of gravity.	4
N/A	**Horizon crossing:** the situation where $k\eta = 1$.	47
N/A	**Horizon problem (Homogeneity problem):** a cosmological problem in which the CMB appears homogeneous despite the comoving horizon exceeding the comoving Hubble radius.	10
H	**Hubble rate:** a parameter characterising the variation of a with respect to energy.	7
ϵ_H and τ_H	**Hubble slow-roll parameters:** slow-roll parameters written in terms of the Hubble rate H.	44
H_0	**Hubble's constant:** the constant of proportionality in Hubble's law.	9
$v = H_0 D$	**Hubble's law:** a law that encapsulates the proportional relationship between the distance of galaxies from Earth and their recessional velocities.	9
N/A	**Inflation (cosmic expansion):** a period in which the scale factor undergoes a rapidly accelerated expansion driven by negative pressure.	5
φ	**Inflation (scalar field):** the source object of the inflationary expansion.	13
$\frac{dx}{d\varphi}$ or x_φ	**Inflation derivative:** the variation of an arbitrary variable x with respect to the scalar field inflation φ.	14
N/A	**Inflationary model:** "a physical model which can lead to inflationary solutions" [46].	13
N/A	**Inflationary scenario:** "a description of the universe which involves a period of inflation" [46].	13
N/A	**Leptogenesis:** the hypothetical process responsible for the excess of leptons over antileptons in the universe.	19
N/A	**Matter-dominated epoch:** A cosmological epoch in which non-relativistic matter contributions dominate the energy density and causes the scale factor to vary as $a \propto t^{2/3}$.	7
$\delta g_{\mu\nu}$	**Metric perturbations:** a small perturbative expansion around the homogeneous FRW metric at first-order.	19
N/A	**Mukhanov-Sasaki equation:** an equation that takes the form of a harmonic oscillator with a time-dependent frequency	45

Notation	Definition	Page
G_N	**Newton's gravitational constant** with a value of $6.67 \times 10^{-11}\text{Nm}^2\text{kg}^{-2}$) and set to 1 for the Friedmann equations.	8
Ψ	**Newtonian potential:** one of the scalar functions contributing to the scalar perturbations in the FRW metric.	21
N/A	**Origin of large-scale structure problem:** the cosmological problem regarding the generation of primordial perturbations which later formed the structure of the universe.	19
Θ_0	**Perturbations to the distribution function** integrated over all directions which contributes to the energy density of photons and anisotropic stress.	32
$\mathcal{N}_0$	**Perturbations to the neutrino distribution** which contributes to the energy density of neutrinos and the anisotropic stress.	32
$x = \bar{x} + \delta x$	**Perturbed redefinition:** a redefinition of arbitrary object x as its perturbed version with $\bar{x}$ as its homogeneous expression and δx its perturbations.	19
m_{Pl}	**Planck mass:** mass in terms of Planck units.	44
$V(\varphi)$	**Potential energy of inflation:** the potential energy of the inflation scalar field φ.	13
ϵ_V and τ_V	**Potential slow-roll parameters:** slow-roll parameters written in terms of *varphi*'s potential $V(\varphi)$.	44
$\mathcal{P}_q(k)$	**Power spectrum** of an arbitrary observable q in terms of its Fourier modes k.	46
P	**Pressure:** the force exerted perpendicularly on an object per unit area of the object's surface on which it is distributed.	9
N/A	**Primordial Gravitational waves (PGWs):** gravitational waves produced by primordial tensor perturbations in the metric during inflation.	5
$\left(k_i k_j - \frac{\delta_{ij}}{3}\right)$	**Projection operator:** an operator which extracts the longitudinal traceless part of an a tensor.	31
N/A	**Radiation-dominated epoch:** A cosmological epoch in which radiation energy dominates and causes the scale factor to vary as $a \propto t^{1/2}$.	7
N/A	**Red-tilted spectrum** a term used to describe when the observed spectral indices are less than unity	51
$f(\eta\vec{x})$	**Redefined field:** a redefinition used in the derivation of φ's action.	45
$\bar{h}$	**Reduced Planck constant:** the reduced Planck constant divided by 2π and set to 1 throughout the dissertation.	44
M_{Pl}	**Reduced Planck mass:** the Planck mass divided by $\sqrt{8\pi}$.	44
$\mathcal{R}$	**Ricci scalar:** the simplest curvature invariant of a Riemannian manifold which can be derived from contracting both indices in the Ricci tensor with the metric.	8
$R_{\gamma\nu}$	**Ricci tensor:** a rank-2 tensor that represents the difference between a volume in curved space and in Euclidean space.	8
α_s	**Running of the scalar spectral index:** a parameter that characterises deviations from a scale-invariant spectrum.	51
$\phi\ \psi\ B\ E$	**Scalar functions** characterising scalar perturbations about the FRW metric which are linked to the energy density.	20
n_s	**Scalar spectral index:** a parameter characterising energy density variation with respect to the scale.	47

Notation	Definition	Page
$a(t)$	**Scale factor:** a parameter characterising the expansion of the universe with cosmic time.	5
N/A	**Scale-invariant spectrum:** a term used to describe when the observed spectral indices equal unity	51
N/A	**Second quantisation method:** the formalism used to describe and analyse quantum many-body systems	45
N/A	**Slow-roll approximation model:** an inflationary model in which the scalar field φ rolls slowly down its potential $V(\varphi)$ such that it never reaches its true vacuum within the time frame of interest.	14
ϵ and τ	**Slow-roll parameters:** a couple of parameters that characterise the slow-roll approximation model.	14
ds^2	**Spacetime interval:** an invariant distance in spacetime.	7
Φ	**Spatial curvature:** one of the scalar functions contributing to the scalar perturbations in the FRW metric.	21
$\frac{\partial x}{\partial k^i} or x_{,i}$	**Spatial derivative (Fourier space):** the variation of an arbitrary variable x with respect to the spatial coordinate in Fourier space k^i.	24
N/A	**Spatially-flat slicing gauge:** a gauge choice in which the g_{ij} components of the FRW metric is unperturbed.	21
c	**Speed of light** with a value of $3 \times 10^8 \text{ms}^{-1}$ and set to 1 throughout the dissertation.	8
N/A	**Stochastic gravitational waves:** a superposition of gravitational waves from independent sources coming from all directions which are seen as noise on a gravitational wave-detecor.	56
N/A	**Sub-horizon scale:** the limit where $k\eta << 1$.	47
N/A	**Super-horizon scale:** the limit where $k\eta >> 1$.	47
N/A	**Synchronous gauge:** a gauge choice that uses "a coordinate system in which the metric is fitted to a set of imagined geodesically and irrotationally moving observers" [25].	21
n_t	**Tensor spectral index:** a parameter used to characterise the power spectrum of the tensor perturbations	49
r	**Tensor-to-scalar ratio:** the ratio between the scalar and tensor power spectra.	49
$\frac{dx}{d\eta}$ or x'	**Time derivative (conformal time):** the variation of an arbitrary variable x with respect to conformal time η.	20
$\frac{dx}{dt}$ or $\dot{x}$ or $x_{,0}$	**Time derivative (cosmic time):** the variation of an arbitrary variable x with respect to cosmic time t.	7
$\mathcal{W}(f_k^* f_k)$	**Wronskian:** a determinant used in the study of differential equations which may have a linear-dependence on a set of solutions	46

2 Primordial Perturbations during Inflation

This section introduces the primordial perturbations generated during inflation. It starts by addressing the problem related to the origins of the large-scale structure of the universe using the theory of inflation followed by introducing the metric perturbations and their classifications.

2.1 Origin of the Large-Scale Structure

Despite the notion of a homogeneous and isotropic universe, there was much scepticism surrounding its consistency with regards to the formation of galaxy clusters making up the structure of the universe, as the process involves gravitationally-bound overdensities to collapse in an initial density field [39] during the matter-dominated epoch. Such density imbalance indicates an inhomogeneous universe instead. In fact, the overdensities that led to such a structure are suggested to have originated from small density fluctuations which had formed in the same primordial plasma where baryogenesis[17] and leptogenesis[18] are thought to have occurred [42]. Measurements of anisotropies in the CMB since its first discovery further support this [12, 15].

The problem with the origin of the large-scale structure is that the hot Big Bang model could not account for the formation of these small density fluctuations at primordial-level. In fact, the problem is linked to the horizon/homogeneity problem previously explained in subsubsection 1.2.2. Assuming the production of these inhomogeneities require a causal physical process, they should not appear in the CMB, whose regions are considered causally-disconnected in the absence of an additional evolutionary epoch [42]. In another approach, one could extrapolate back in time to the point of singularity and show that these inhomogeneities could not have been produced in a causal physical process as they would have existed well beyond the horizon [42].

Similarly to the horizon/homogeneity problem, there is much need for an additional physical process to explain the large-scale structure of the universe. Shortly after its introduction by works in 1981 and 1982 to address the horizon/homogeneity problem, flatness problem and monopole problem [7, 30, 44], many realised the theory of inflation to simultaneously solve the origin of the large-scale structure problem as well[19] [13, 31, 32, 64]. In the inflationary scenario, cosmological scales of interest achieved uniformity in a causal region within the horizon before expanding at an accelerated rate after which it exceeds the horizon by an order of 10^{28}. Thus, it is reasonable to propose that the inhomogeneities observed in the CMB were generated in the same causal region and later stretched to cosmic scales, assuming their amplitudes were preserved during the expansion.

In this section, we consider the primordial fluctuations as small perturbations expanded around the homogeneous and isotropic universe introduced in subsection 1.2.1. We do this by adding perturbations to the FRW metric. Since the observed fluctuations in the CMB are of the order 10^{-5}, their initial primordial values are predicted to be much smaller. For this reason, it is sufficient to only consider them at first-order,

$$g_{\mu\nu} = \bar{g}_{\mu\nu} + \delta g_{\mu\nu}, \tag{2.1}$$

[17] Baryogenesis refers to the process responsible for the excess of baryonic matter over baryonic antimatter in the universe.

[18] Leptogenesis refers to the hypothetical process responsible for the excess of leptons over antileptons in the universe.

[19] This makes the theory of inflation a cornerstone in modern cosmology.

where now we relabel the FRW metric in equation (1.2) as $\bar{g}_{\mu\nu}$, redefine $g_{\mu\nu}$ as the overall perturbed FRW metric, and denote $\delta g_{\mu\nu}$ as its first-order perturbation. Note that $\bar{g}_{\mu\nu} >> \delta g_{\mu\nu}$. The following subsection will specify the perturbations of interest.

2.2 Metric Perturbations during Inflation

2.2.1 Classification of Metric Perturbations

Following the perturbed FRW metric introduced in the previous subsection, its general spacetime interval is given by

$$ds^2 = (\bar{g}_{\mu\nu} + \delta g_{\mu\nu})dx^\mu dx^\nu. \tag{2.2}$$

Since symmetry properties of the homogeneous background are invariant under spatial rotations and translations, they are used to distinguish the perturbations present in the metric [47]. There are three types of metric perturbations; scalar, vector and tensor. It is useful to explore these perturbations in conformal time, though their expressions in the conformal Newtonian gauge will be reverted back to cosmic time to ease the calculations Section 3.

Scalar Perturbations The scalar perturbations are made up of four scalar functions, ϕ, ψ, B and E, which are generated from energy density inhomogeneities. In their presence, the spacetime interval in equation (2.2) becomes:

$$\mathrm{ds}^2 = a^2[-(1+2\phi)\mathrm{d}\eta^2 + 2B_{,i}\mathrm{dx}^\mathrm{i}\mathrm{d}\eta + \{(1+2\psi)\delta_{ij} + 2E_{,ij}\}\mathrm{dx}^\mathrm{i}\mathrm{dx}^\mathrm{j}], \tag{2.3}$$

where $B_i = \frac{\partial B}{\partial x^i}$ and similarly, $E_{,ij} = \frac{\partial E}{\partial x^i \partial x^j}$. To simplify this general form, one can consider their transformations under a change of coordinates, $x^\mu \to \tilde{x}^\mu = x^\mu + \xi^\mu$:

$$\begin{aligned}
\phi \to \tilde{\phi} &= \phi - \frac{1}{a}(a\xi^0)', \\
\psi \to \tilde{\psi} &= \psi + \frac{a'}{a}\xi^0, \\
B \to \tilde{B} &= B + \zeta' - \xi^0, \\
E \to \tilde{E} &= E + \zeta,
\end{aligned}$$

where ζ is a scalar function and the apostrophes indicate derivatives with respect to conformal time, ie. $\zeta' = \frac{d\zeta}{d\eta}$. From these, we have their simplest gauge-invariant linear combinations:

$$\begin{aligned}
\Phi &\equiv \phi - \frac{1}{a}[a(B - E')]', \\
\Psi &\equiv \psi + \frac{a'}{a}(B - E').
\end{aligned} \tag{2.4}$$

Since these functions manifest gravity instability due to their links to the energy density, the scalar perturbations directly contribute to the formation of the large-scale structure of our universe.

Vector Perturbations The simplest form of equation (2.2) in terms of vector perturbations is

$$\mathrm{ds}^2 = a^2[-\mathrm{d}\eta^2 + 2S_i\mathrm{dx}^\mathrm{i}\mathrm{d}\eta + (\delta_{ij} + F_{i,j} + F_{j,i})\mathrm{dx}^\mathrm{i}\mathrm{dx}^\mathrm{j}]. \tag{2.5}$$

In this expression, S_i and F_i are both divergenceless vectors related to rotational motions of fluid that transform as

$$\begin{aligned}
S_i \to \tilde{S}_i &= S_i + \xi'_{\perp i}, \\
F_i \to \tilde{F}_i &= F_i + \xi_{\perp i},
\end{aligned}$$

under a change of coordinates. Note that here, $\xi_{\perp i}$ is a divergenceless 3-vector. While one may form a gauge-invariant linear combination of S_i and F_i, a study of these vector perturbations is uninteresting as they decay very fast and thus play no part in large-scale structure formations. For this reason, we will not consider them in section 3.

Tensor Perturbations The last type of metric perturbations to consider is the tensor perturbations. In this case, equation (2.2) takes the form

$$\mathrm{ds}^2 = a^2[-\mathrm{d}\eta^2 + (\delta_{ij} + \mathcal{H}_{ij})\mathrm{dx}^\mathrm{i}\mathrm{dx}^\mathrm{j}], \tag{2.6}$$

where $\mathcal{H}_{ij}$ is the divergenceless, traceless, symmetric tensor[20] representing GWs travelling in the z-direction:

$$\mathcal{H}_{ij} = \begin{pmatrix} h_+ & h_\times & 0 \\ h_\times & -h_+ & 0 \\ 0 & 0 & 0 \end{pmatrix}. \tag{2.7}$$

Its components, h_+ and $h_\times$, are the degrees of freedom pointing in the $x-y$ plane. $\mathcal{H}_{ij}$ itself is already gauge-invariant, thus the GWs remain the same in all frames of reference. As they are generated during the primordial epoch, they are the PGWs introduced in subsubsection 1.1.2. To date, much research has been dedicated to detecting traces of PGWs in the CMB [10, 29, 38, 72].

2.2.2 Choice of Gauge

It is useful to formulate gauge-invariant expressions of these perturbations as cosmologists adopt different gauge choices (which result in different forms of the FRW metric) for different tasks. For example, a gauge with *spatially flat slicing*[21] results in simple forms of equations for these perturbations, thus it is often used when deriving such equations [23]. On the other hand, cosmologists deploying computational methods in the study of anisotropies and inhomogeneities would prefer the *synchronous gauge*[22] [23].

This dissertation uses the *conformal Newtonian gauge* as the derivations of evolution equations of the metric perturbations in this gauge are quite manageable. Moreover, it caters to a wider audience as its workings are doable for anyone familiar with general relativity. This gauge sets $B = E = 0$, thus from equations in (2.4), we have that $\phi = \Phi$ and $\psi = \Psi$. Thus, the spacetime interval involving the scalar-perturbed FRW metric in this gauge is

$$\mathrm{ds}^2 = a^2[-(1+2\Phi)\mathrm{d}\eta^2 + \{\delta_{ij}(1+2\Psi)\}\mathrm{dx}^\mathrm{i}\mathrm{dx}^\mathrm{j}]. \tag{2.8}$$

Specifically, Ψ corresponds to the Newtonian potential and Φ corresponds to the spatial curvature [23]. To ease the derivation of the EFE for scalar and tensor perturbations in section 3, the FRW metric components for the scalar and tensor perturbations are rewritten using cosmic time, separately.

[20] 'Divergenceless' and 'traceless' here refer to the fact that $k^i\mathcal{H}_{ij} = k^j\mathcal{H}_{ij} = 0$ since $\mathcal{H}_{ij}$ has no components in the z-direction.

[21] A gauge with spatially flat slicing refers to a gauge choice in which the g_{ij} component of the metric is unperturbed [23].

[22] Synchronous gauge refers to a gauge choice that uses "a coordinate system in which the metric is fitted to a set of imagined geodesically and irrotationally moving observers" [25].

Scalar-Perturbed FRW Metric The FRW metric perturbed by scalar perturbations is given by:

$$\begin{aligned} g_{00}(t,\vec{x}) &= -1 - 2\Psi(t,\vec{x}), \\ g_{0i}(t,\vec{x}) &= 0, \\ g_{ij}(t,\vec{x}) &= a^2(t)\delta_{ij}[1 + 2\Phi(t,\vec{x})]. \end{aligned}$$

Tensor-Perturbed FRW Metric The FRW metric perturbed by tensor perturbations comprises of the components,

$$\begin{aligned} g_{00} &= -1, \\ g_{0i} &= 0, \\ g_{ij} &= a^2(t)[\delta_{ij} + \mathcal{H}_{ij}]. \end{aligned}$$

2.2.3 The Decomposition Theorem

Despite the metric perturbations being generated in the same epoch, their three different classes are actually independent of one another, as they obey the *decomposition theorem* [23]. This means that while Φ and Ψ are intertwined, they are not affected by $\mathcal{H}_{ij}$ [23]. We will assume this is true for now, but an actual proof of the theorem will be provided in subsection 3.3 once we have obtained the EFE of the perturbations.

3 The Perturbed Einstein Equations

To understand the physical interpretation of the metric perturbations introduced in section 2.2.1, this section aims to derive the perturbed Einstein equations[23]. Since the metric perturbations obey the decomposition theorem stated in subsubsection 2.2.3, the derivation for the two types of perturbations can be done separately under subsections 3.1 and 3.2.

The set of steps used in these subsections is similar to the ones presented in section 1.2.1:

1. Establish the inverse FRW metric for each case.
2. Calculate the Christoffel symbols, $\Gamma^{\alpha}_{\mu\nu}$.
3. Compute the Ricci tensors, $R_{\mu\nu}$.
4. Deduce the Ricci scalar.
5. Determine the Einstein tensor, $G_{\mu\nu}$ using these values.
6. Complete the EFE by considering the energy-momentum tensor, $T_{\mu\nu}$ for each case.

In step 6, we will reinstate G_N but maintain $c = 1$.

Once obtained, the respective perturbed Einstein equations are summarised at the end of the subsections, along with their physical interpretation. Furthermore, a proof of the decomposition theorem is given in subsection 3.3 using these equations. Note that all workings in this section is guided by Chapter 5 of *Modern Cosmology* by Dodelson, 2003 [23], though elaborated in more detail. Also note that as per subsection 2.1, the following tensors and scalar are redefined:

$$\begin{aligned} G^{\mu}_{\nu} &= \bar{G}^{\mu}_{\nu} + \delta G^{\mu}_{\nu}, \\ R_{\gamma\nu} &= \bar{R}_{\gamma\nu} + \delta R_{\gamma\nu}, \\ \mathcal{R} &= \bar{\mathcal{R}} + \delta\mathcal{R}, \\ T^{\mu}_{\nu} &= \bar{T}^{\mu}_{\nu} + \delta T^{\mu}_{\nu}, \end{aligned} \tag{3.1}$$

where the bars indicate the homogeneous results obtained in subsubsection 1.2.1 and the delta terms represent contributions from the perturbations.

[23] This refers to the same EFE derived in subsubsection 1.2.1 but with the inclusion of the metric perturbations in subsubsection 2.2.2.

3.1 Scalar Perturbations

This subsection comprises the steps in deriving the Einstein equations perturbed by the scalar perturbations.

3.1.1 The Inverse Scalar-Perturbed FRW Metric

From the scalar-perturbed FRW metric stated in subsubsection 2.2.2, one can obtain its inverse form by inverting the components and applying the Taylor series expansion[24], $\frac{1}{1-x} \approx 1 + x + x^2 + x^3 + ...$ where the perturbations are only considered at first-order. Thus, the components of the inverse FRW metric perturbed by scalar perturbations are

$$\begin{aligned} g^{00}(t,\vec{x}) &= -1 + 2\Psi(t,\vec{x}), \\ g^{0i}(t,\vec{x}) &= 0, \\ g^{ij}(t,\vec{x}) &= \frac{\delta_{ij}}{a^2(t)}[1 - 2\Phi(t,\vec{x})]. \end{aligned} \tag{3.2}$$

In the subsequent subsubsections, the temporal and spatial dependence is assumed but their explicit expressions are dropped to avoid cluttering.

3.1.2 Christoffel Symbols

Recall the formula for the Christoffel symbol in equation (1.9) but with $g_{\mu\nu}$ now defining the scalar-perturbed FRW metric. Firstly, consider **Case 1**, where $\alpha = 0$. Equation (1.9) becomes

$$\Gamma^0_{\mu\nu} = \frac{1}{2} g^{0\gamma}(g_{\gamma\mu,\nu} + g_{\gamma\nu,\mu} - g_{\mu\nu,\gamma}).$$

For non-zero values, γ must be 0 and the equation transforms again as

$$\Gamma^0_{\mu\nu} = \frac{1}{2} g^{00}(g_{0\mu,\nu} + g_{0\nu,\mu} - g_{\mu\nu,0}). \tag{3.3}$$

Note that the subscript $,0$ indicates a derivative with respect to cosmic time, t. Now, apply the different values of μ and ν.

Case 1.1 When $\mu = \nu = 0$, the three terms in the parentheses are $g_{00,0}$, thus only one survives. Based on the first line in equation (3.2), $g_{00,0} = -2\Psi_{,0}$ and so the Christoffel symbol becomes

$$\Gamma^0_{00} = \frac{-1 + 2\Psi}{2}(-2\Psi_{,0}) = \Psi_{,0} - 2\Psi_{,0}\Psi.$$

Case 1.2 Next, consider the values $\mu = 0, \nu = i$. The Christoffel symbol becomes

$$\Gamma^0_{0i} = \frac{-1 + 2\Psi}{2}(g_{00,i} + g_{0i,0} - g_{0i,0}).$$

In the parentheses, the last two terms are just zero, leaving only the first term, $g_{00,i} = -2\Psi_{,i}$. This gives the result,

$$\Gamma^0_{0i} = \frac{-1 + 2\Psi}{2}(-2\Psi_{,i}) = \Psi_{,i} - 2\Psi_{,i}\Psi = \mathrm{i}k_i\Psi - \mathrm{i}2k_i\Psi^2,$$

where in the last equality, we switched to Fourier space, $\Psi_{,i} = \frac{\partial\Psi}{\partial k^i}$. Note that the italicised i labels the spatial component whereas i is the imaginary number possessing the property, $\mathrm{i}^2 = -1$.

[24] This step is permissible since the metric perturbations are very small.

Case 1.3 The last values to consider for this case are $\mu = i$ and $\nu = j$ (or vice versa):

$$\Gamma^0_{ij} = \frac{-1+2\Psi}{2}(g_{0i,j} + g_{0j,i} - g_{ij,0}).$$

The first two terms in the parentheses equal zero, leaving only the third, $-g_{ij,0} = -\delta_{ij}\frac{\partial}{\partial t}a^2(1+2\Phi)$. By applying the product rule to both terms,

$$\delta_{ij}\frac{\partial}{\partial t}a^2 = 2\delta_{ij}\dot{a}a,$$
$$2\delta_{ij}\frac{\partial}{\partial t}(a^2\Phi) = 4\delta_{ij}\dot{a}a\Phi + 2\delta_{ij}a^2\Phi_{,0},$$

the Christoffel symbol up to first-order is

$$\Gamma^0_{ij} = \delta_{ij}\dot{a}a - 2\Psi\delta_{ij}\dot{a}a + 2\delta_{ij}\dot{a}a\Phi + \delta_{ij}a^2\Phi_{,0}.$$

Using the definition for the Hubble rate, $H = \frac{\dot{a}}{a}$, it can be further simplified into

$$\Gamma^0_{ij} = \delta_{ij}a^2(H + 2H(\Phi - \Psi) + \Phi_{,0}).$$

Next, consider **Case 2**, when $\alpha = i$. In this case, equation (1.9) becomes

$$\Gamma^i_{\mu\nu} = \frac{1}{2}g^{i\gamma}(g_{\gamma\mu,\nu} + g_{\gamma\nu,\mu} - g_{\mu\nu,\gamma}).$$

For non-zero values, γ must be l and the equation transforms again as

$$\Gamma^i_{\mu\nu} = \frac{1}{2}g^{il}(g_{l\mu,\nu} + g_{l\nu,\mu} - g_{\mu\nu,l}). \tag{3.4}$$

Now, apply the values of μ and ν, as before.

Case 2.1 When $\mu = \nu = 0$, the Christoffel symbol becomes

$$\Gamma^i_{00} = \frac{1}{2}g^{il}(g_{l0,0} + g_{l0,0} - g_{00,l}).$$

From equation (3.2), the first two terms in the parentheses are zero, leaving only $-g_{00,l} = 2\Psi_{,l}$ in the expression,

$$\begin{aligned}\Gamma^i_{00} &= \frac{1}{2}\left[\frac{\delta_{il}}{a^2}(1-2\Phi)\right][2\Psi_{,l}] \\ &= \frac{\delta_{il}}{a^2}(\Psi_{,l} - 2\Phi\Psi_{,l}) \\ &= \frac{\mathrm{i}k^i}{a^2}\Psi,\end{aligned}$$

where in the last line, $l = i$ and the second-order term was omitted.

Case 2.2 Now, for the case of $\mu = 0$ and $\nu = j$:

$$\Gamma^i_{0j} = \frac{1}{2}\left[\frac{\delta_{il}}{a^2}(1-2\Phi)\right](g_{l0,j} + g_{lj,0} - g_{0j,l}). \tag{3.5}$$

Only the second term in the second parentheses, $g_{lj,0}$ is non-zero, and using the product rule as per the previous working for Γ^0_{0i},

$$g_{lj,0} = 2\delta_{lj}\dot{a}a + 4\delta_{lj}\dot{a}a\Phi + 2\delta_{lj}a^2\Phi_{,0}.$$

By setting $l = j$, the Christoffel symbol becomes

$$\Gamma^i_{0j} = \frac{\delta_{ij}}{a^2}[\dot{a}a + 2\dot{a}a\Phi + a^2\Phi_{,0} - 2\dot{a}a\Phi - 4\dot{a}a\Phi^2 - 2a^2\Phi\Phi_{,0}].$$

To first-order, the final result is

$$\Gamma^i_{0j} = \delta_{ij}\left[\frac{\dot{a}}{a} + \Phi_{,0}\right] = \delta_{ij}(H + \Phi_{,0}).$$

Case 2.3 Lastly, consider the values $\mu = j$, $\nu = k$:

$$\Gamma^i_{jk} = \frac{1}{2}\left[\frac{\delta_{il}}{a^2}(1 - 2\Phi)\right](g_{lj,k} + g_{lk,j} - g_{jk,l}).$$

Since the three terms in the second parentheses are of a similar form, it is enough to work out one of them and apply the same result to the rest by changing indices. Taking the first term as an example,

$$g_{lj,k} = a^2\frac{\partial}{\partial k^k}(\delta_{lj} + 2\delta_{lj}\Phi) = 2\delta_{lj}\Phi_{,k},$$

and applying the result to the second and third terms, the Christoffel symbol becomes

$$\Gamma^i_{jk} = \delta_{il}(1 - 2\Phi)[\delta_{lj}\Phi_{,k} + \delta_{lk}\Phi_{,j} - \delta_{jk}\Phi_{,l}].$$

After eliminating the delta function outside the parentheses by setting $l = i$, expanding the brackets and neglecting the second-order terms, the result is

$$\Gamma^i_{jk} = i\Phi(\delta_{ij}k_k + \delta_{ik}k_j - \delta_{jk}k_i).$$

Summary To summarise, all the non-zero scalar-perturbed Christoffel symbols up to first-order are:

$$\begin{aligned}
\Gamma^0_{00} &= \Psi_{,0}, \\
\Gamma^0_{0i} &= \mathrm{i}k_i\Psi, \\
\Gamma^0_{ij} &= \delta_{ij}a^2(H + 2H(\Phi - \Psi) + \Phi_{,0}), \\
\Gamma^i_{00} &= \frac{\mathrm{i}k^i}{a^2}\Psi, \\
\Gamma^i_{0j} &= \delta_{ij}(H + \Phi_{,0}), \\
\Gamma^i_{jk} &= i\Phi(\delta_{ij}k_k + \delta_{ik}k_j - \delta_{jk}k_i).
\end{aligned} \tag{3.6}$$

With these values, one can proceed to compute the scalar perturbed Ricci tensors, $R_{\gamma\nu}$ in the next subsubsection.

3.1.3 Ricci Tensors

Recall the definition of the Ricci tensor, $R_{\mu\nu}$ stated in equation (1.7). Finding $R_{\gamma\nu}$ is crucial as it is needed to determine the perturbed Ricci scalar, $\mathcal{R}$ and hence, the Einstein tensor, G^{μ}_{ν}. Based on the definition of G^{μ}_{ν} in equation (1.6), it is sufficient to determine only R_{00} and R_{ij} since $g^{0i} = 0$ and $g_{0i} = 0$, therefore its corresponding Einstein tensor will equal to zero. By substituting in the non-zero Christoffel symbols summarised in equation (3.6), $R_{\gamma\nu}$ will automatically account for the scalar perturbations.

Case 1 When $\gamma = \nu = 0$, the Ricci tensor takes the form:

$$R_{00} = \Gamma^{\alpha}_{00,\alpha} - \Gamma^{\alpha}_{0\alpha,0} + \Gamma^{\alpha}_{\beta\alpha}\Gamma^{\beta}_{00} - \Gamma^{\alpha}_{\beta 0}\Gamma^{\beta}_{0\alpha}. \tag{3.7}$$

Now, apply the different values of α and later, β.

Case 1.1 When $\alpha = 0$, $R_{00} = 0$ as the four terms cancel each other,

$$R_{00} = \Gamma^{0}_{00,0} - \Gamma^{0}_{00,0} + \Gamma^{0}_{\beta 0}\Gamma^{\beta}_{00} - \Gamma^{0}_{\beta 0}\Gamma^{\beta}_{00}.$$

Case 1.2 Consider the four terms separately when $\alpha = i$:

$$R_{00} = \Gamma^{i}_{00,i} - \Gamma^{i}_{0i,0} + \Gamma^{i}_{\beta i}\Gamma^{\beta}_{00} - \Gamma^{i}_{\beta 0}\Gamma^{\beta}_{0i}.$$

The first term is evaluated as:

$$\Gamma^{i}_{00,i} = \frac{\partial}{\partial k^i}\left(\frac{\mathrm{i}k^i}{a^2}\Psi\right) = -\frac{k^2}{a^2}\Psi$$

The second one involves differentiating two terms, $-\Gamma^{i}_{0i,0} = -3\frac{\partial}{\partial t}\left(H + \Phi_{,0}\right)$[25]:

$$\frac{\partial}{\partial t}(\dot{a}a^{-1}) = \frac{\ddot{a}}{a} - H^2,$$
$$\frac{\partial}{\partial t}\Phi_{,0} = \Phi_{,00}.$$

Hence, $-\Gamma^{i}_{0i,0} = -3\left(\frac{\ddot{a}}{a} - H^2 + \Phi_{,00}\right)$.

The third term, $\Gamma^{i}_{\beta i}\Gamma^{\beta}_{00}$, is more complicated as now, one needs to consider the possible values of β, as well. If $\beta = 0$, the term becomes

$$\Gamma^{i}_{0i}\Gamma^{0}_{00} = [3(H + \Phi_{,0})][\Psi_{,0}].$$

Whereas if $\beta = j$, it becomes

$$\Gamma^{i}_{ji}\Gamma^{j}_{00} = [\mathrm{i}3k_j\Phi][\frac{\mathrm{i}k^j}{a^2}\Psi].$$

Since the latter option results in a second-order term, only the former will be considered.

Similarly, the option of $\beta = 0$ is ignored for the fourth term as it results in an overall second-order term. Thus, to first-order, it is

$$-\Gamma^{i}_{j0}\Gamma^{j}_{0i} \equiv -3(H^2 + 2H\Phi_{,0}).$$

Summary Therefore, the overall temporal Ricci tensor, R_{00} is given by:

$$R_{00} = -3\frac{\ddot{a}}{a} - \frac{k^2}{a^2}\Psi - 3\Phi_{,00} + 3H(\Psi_{,0} - 2\Phi_{,0}). \tag{3.8}$$

[25]The 3 comes from the implicit sum of δ_{ii} in $\Gamma^{i}_{0j,0}$.

Case 2 When $\gamma = i$ and $\nu = j$, the Ricci tensor takes the form:

$$R_{ij} = \Gamma^{\alpha}_{ij,\alpha} - \Gamma^{\alpha}_{i\alpha,j} + \Gamma^{\alpha}_{\beta\alpha}\Gamma^{\beta}_{ij} - \Gamma^{\alpha}_{\beta j}\Gamma^{\beta}_{i\alpha}. \tag{3.9}$$

Case 2.1 Now, consider $\alpha = 0$. The above equation becomes

$$R_{ij} = \Gamma^{0}_{ij,0} - \Gamma^{0}_{i0,j} + \Gamma^{0}_{\beta 0}\Gamma^{\beta}_{ij} - \Gamma^{0}_{\beta j}\Gamma^{\beta}_{i0}. \tag{3.10}$$

The first term is just a first-order time derivative of Γ^{0}_{ij},

$$\begin{aligned}\Gamma^{0}_{ij,0} &= \delta_{ij}\frac{\partial}{\partial t}[a^2H + 2a^2H\Phi - 2a^2H\Psi + a^2\Phi_{,0}] \\ &= \delta_{ij}(\dot{a}^2 + \ddot{a}a + 2\dot{a}^2\Phi + 2\ddot{a}a\Phi + 2\dot{a}a\Phi_{,0} - 2\dot{a}^2\Psi - 2\ddot{a}a\Psi - 2\dot{a}a\Psi_{,0} + 2\dot{a}a\Psi_{,0} + a^2\Psi_{,00}).\end{aligned}$$

By reinstating the definition $\dot{a} = Ha$, this result is simplified as

$$\Gamma^{0}_{ij,0} = \delta_{ij}(a^2H^2 + a\ddot{a} + 2a^2H^2\Phi + 2a\ddot{a}\Phi + 4a^2H\Phi_{,0} - 2a^2H^2\Psi - 2a\ddot{a}\Psi - 2a^2H\Psi_{,0} + a^2\Phi_{,00}).$$

Similarly, to get the second term, a spatial derivative is operated on $-\Gamma^{0}_{i0}$:

$$-\Gamma^{0}_{i0,j} = -\frac{\partial}{\partial k^j}[\mathrm{i}k_i\Psi] = -\mathrm{i}^2k_ik_j\Psi = k_ik_j\Psi.$$

Now, we expand the third term in values of β,

$$\Gamma^{0}_{\beta 0}\Gamma^{\beta}_{ij} = \Gamma^{0}_{00}\Gamma^{0}_{ij} + \Gamma^{0}_{l0}\Gamma^{l}_{ij},$$

where in the former term, $\beta = 0$ and in the latter, $\beta = l$. By recalling the non-zero Christoffel symbols summarised in equation (3.6), we can neglect the $\beta = l$ term as it contains only second-order terms. On the other hand, we can work out the $\beta = 0$ term by performing the product,

$$\Gamma^{0}_{00}\Gamma^{0}_{ij} = [\Psi_{,0}][\delta_{ij}(a^2H + 2a^2H\Phi - 2a^2H\Psi + a^2\Phi_{,0})].$$

After only considering up to first-order, the third term in equation (3.10) is just:

$$\Gamma^{0}_{00}\Gamma^{0}_{ij} = \delta_{ij}a^2H\Psi_{,0}.$$

We repeat the expansion for the fourth term,

$$-\Gamma^{0}_{\beta j}\Gamma^{\beta}_{i0} = -\Gamma^{0}_{0j}\Gamma^{0}_{i0} - \Gamma^{0}_{lj}\Gamma^{l}_{i0},$$

where we ignore the $\beta = 0$ term as we are only interested in the perturbations up to first-order. The product in the $\beta = l$ term is given by

$$-\Gamma^{0}_{lj}\Gamma^{l}_{i0} = -[\delta_{lj}a^2(H + 2H(\Phi - \Psi) + \Phi_{,0})][\delta_{li}(H + \Phi_{,0})].$$

Putting aside the second-order terms, the fourth term of equation (3.10) is:

$$-\Gamma^{0}_{lj}\Gamma^{l}_{i0} = \delta_{ij}(a^2H^2 + 2a^2H^2\Phi - 2a^2H^2\Psi + 2a^2H\Phi_{,0}).$$

Case 2.2 In this case, consider $\alpha = k$. Equation (3.9) transforms as

$$R_{ij} = \Gamma^{k}_{ij,k} - \Gamma^{k}_{ik,j} + \Gamma^{k}_{\beta k}\Gamma^{\beta}_{ij} - \Gamma^{k}_{\beta j}\Gamma^{\beta}_{ik}. \tag{3.11}$$

The first term is a derivative of Γ^{k}_{ij} with respect to k^k. Performing the derivative gives

$$\Gamma^{k}_{ij,k} = -\Phi(\delta_{ki}k_jk_k + \delta_{kj}k_ik_j - \delta_{ij}k_kk_k) = \delta_{ij}k^2\Phi - 2k_ik_j\Phi,$$

where in the last equality, we set $k = i$ and later, $j = i$.

While the second term in equation (3.11) takes a similar form as the first, summing over k leads to only one term surviving in the bracket of Γ^k_{ik}, giving:

$$-\Gamma^k_{ik,j} = -\mathrm{i}3\frac{\partial}{\partial k^j}[k_i\Phi] = 3k_ik_j\Phi.$$

For the third term in equation (3.11), it is sufficient to only consider $\beta = 0$, since $\beta = l$ results in second-order terms. Thus, we have the following product,

$$\Gamma^0_{0k}\Gamma^0_{ij} = \delta_{kk}[H + \Phi_{,0}][\delta_{ij}(a^2H + 2a^2H\Phi - 2a^2H\Psi + a^2\Phi_{,0})],$$

whose final result up to first-order is given by

$$\Gamma^k_{0k}\Gamma^0_{ij} = 3\delta_{ij}a^2(H^2 + 2H^2\Phi - 2H^2\Psi + 2H\Phi_{,0}).$$

The same is done for the fourth term - setting $\beta = l$ leads to second-order terms, hence they are negligible. This leaves us with the $\beta = 0$ term,

$$-\Gamma^k_{0j}\Gamma^0_{ik} = -[\delta_{kj}(H + \Phi_{,0})][\delta_{ik}(a^2H + 2a^2H\Phi - 2a^2H\Psi + a^2\Phi_{,0})],$$

whose answer containing only zero-order and first-order terms, is

$$-\Gamma^k_{0j}\Gamma^0_{ik} = -\delta_{ij}a^2(H^2 + 2H^2\Phi - 2H^2\Psi + 2H\Phi_{,0}).$$

Summary Putting together all the results we have obtained in **Case 2.1** and **Case 2.2**, the Ricci tensor perturbed by scalar perturbations, R_{ij} is given by

$$R_{ij} = \delta_{ij}(2a^2H^2+a\ddot{a}+4a^2H^2\Phi-4a^2H^2\Psi+2a\ddot{a}\Phi-2a\ddot{a}\Psi+6a^2H\Phi_{,0}-a^2H\Psi_{,0}+a^2\Phi_{,00}+k^2\Phi)+k_ik_j(\Phi+\Psi).$$

This expression is further simplified into:

$$R_{ij} = \delta_{ij}\left[(2a^2H^2 + \ddot{a}a)(1 + 2\Phi - 2\Psi) + a^2H(6\Phi_{,0} - \Psi_{,0}) + a^2\Phi_{,00} + k^2\Phi\right] + k_ik_j(\Phi + \Psi). \tag{3.12}$$

3.1.4 The Ricci Scalar

After computing the Ricci tensors, one can now proceed to deduce the perturbed Ricci scalar, $\mathcal{R}$. Referring to the definition of $\mathcal{R}$ given in equation (1.8), this computation is divided into two parts.

Part 1

$$g^{00}R_{00} = [-1+2\Psi]\left[-3\frac{\ddot{a}}{a} - \frac{k^2}{a^2}\Psi - 3\Phi_{,00} + 3H(\Psi_{,0} - 2\Phi_{,0})\right]$$

Part 2

$$g^{ij}R_{ij} = \left[\frac{1-2\Phi}{a^2}\right]\left[3\{(2a^2H^2 + \ddot{a}a)(1+2\Phi-2\Psi) + a^2H(6\Phi_{,0} - \Psi_{,0}) + a^2\Phi_{,00} + k^2\Phi\} + k^2(\Phi+\Psi)\right]$$

Part 1 consists of 10 terms whereas **Part 2** comprises of 24 terms altogether, hence they are not written explicitly here. Summing the two parts gives the scalar-perturbed Ricci scalar, $\mathcal{R}$ up to first-order:

$$\mathcal{R} = 6\left(\frac{\ddot{a}}{a} + H^2\right) - 12\Psi\left(\frac{\ddot{a}}{a} + H^2\right) + 2\frac{k^2}{a^2}\Psi + 6\Phi_{,00} - 6H(\Psi_{,0} - 4\Phi_{,0}) + 4\frac{k^2}{a^2}\Phi. \tag{3.13}$$

Note that the first two terms are the zero-order terms, $\bar{\mathcal{R}}$ which match exactly as those found in the Friedmann equations' derivation, where scalar perturbations were absent.

3.1.5 The Einstein Tensor

This subsubsection aims to complete Step 5 - determining the Einstein tensor, G^{μ}_{ν} defined in equation (1.6). Using R_{00}, R_{ij} and $\mathcal{R}$, the temporal, G^0_0 and spatial, G^i_j parts of the Einstein tensor are computed separately in the following parts:

Part 1: Temporal Part

$$\begin{aligned} G^0_0 &= g^{00}R_{00} - \frac{1}{2}g^{00}g_{00}\mathcal{R} \\ &= (-1+2\Psi)R_{00} - \frac{\mathcal{R}}{2}. \end{aligned}$$

By only considering up to first-order terms, they consist of:

$$\begin{aligned} (-1+2\Psi)R_{00} &= 3\frac{\ddot{a}}{a} - 6\Psi\frac{\ddot{a}}{a} + \frac{k^2}{a^2}\Psi + 3\Phi_{,00} - 3H\Psi_{,0} + 6H\Phi_{,0}, \\ \frac{\mathcal{R}}{2} &= -3\frac{\ddot{a}}{a} - 3H^2 + 6\Psi H^2 + 6\Psi\frac{\ddot{a}}{a} - \frac{k^2}{a^2}\Psi - 3\Phi_{,00} + 3H\Psi_{,0} - 12H\Phi_{,0} - 2\frac{k^2}{a^2}\Phi. \end{aligned}$$

Their total sum gives:

$$G^0_0 = -3H^2 + 6\Psi H^2 - 6H\Phi_{,0} - 2\frac{k^2}{a^2}\Phi.$$

Part 2: Spatial Part

$$\begin{aligned} G^i_j &= g^{ik}R_{kj} - g^{ik}g_{ik}\mathcal{R} \\ &= \frac{\delta^{ik}(1-2\Phi)}{a^2}R_{kj} - \frac{\delta_{ij}}{2}\mathcal{R}, \end{aligned}$$

where up to first-order,

$$\begin{aligned} \frac{\delta^{ik}(1-2\Phi)}{a^2}R_{kj} =& \frac{\delta_{ij}}{a^2}\left[\left\{(2a^2H^2+a\ddot{a})(1+2\Phi-2\Psi)+a^2H(6\Phi_{,0}-\Psi_{,0})+a^2\Phi_{,00}+k^2\Phi\right\}\right] \\ &+\delta_{ij}[2\Phi(-2a^2H^2-a\ddot{a})]+\frac{k_ik_j(\Phi+\Psi)}{a^2} \end{aligned}$$

and

$$\frac{\delta_{ij}}{2}\mathcal{R} = \delta_{ij}\left[3\left(H^2+\frac{\ddot{a}}{a}\right)-6\Psi\left(H^2+\frac{\ddot{a}}{a}\right)+\frac{k^2}{a^2}\Psi+3\Phi_{,00}-3H(\Psi_{,0}-4\Phi_{,0})+2\frac{k^2}{a^2}\Phi\right].$$

Summing the two together, the spatial part of the Einstein tensor is given by

$$G^i_j = A\delta_{ij} + \frac{k_ik_j(\Phi+\Psi)}{a^2}, \tag{3.14}$$

where A is:

$$\begin{aligned} A =& \frac{1}{a^2}\left[\left\{(2a^2H^2+a\ddot{a})(1+2\Phi-2\Psi)+a^2H(6\Phi_{,0}-\Psi_{,0})+a^2\Phi_{,00}+k^2\Phi\right\}-2\Phi(2a^2H^2+a\ddot{a})\right] \\ &+3\left(-H^2+\frac{\ddot{a}}{a}\right)+6\Psi\left(H^2-\frac{\ddot{a}}{a}\right)-\frac{k^2}{a^2}\Psi-3\Phi_{,00}+3H(\Psi_{,0}+4\Phi_{,0})-2\frac{k^2}{a^2}\Phi. \end{aligned}$$

While A contributes to G^i_j, its terms would lead to a very complicated form of the Einstein equation. A neat trick to simplify the equations is to exclude A by picking out the longitudinal, traceless part of G^i_j. We do this by operating the *projection operator*, $\left(k_ik_j - \frac{\delta_{ij}}{3}\right)$ on equation (3.14) [23]. The projection operator causes to all terms proportional to δ_{ij} to equal to zero, and hence:

$$\left(k_ik_j-\frac{\delta_{ij}}{3}\right)G^i_j = \left(k_ik_j-\frac{\delta_{ij}}{3}\right)\left(\frac{k_ik_j(\Phi+\Psi)}{a^2}\right) = \frac{2}{3a^2}k^2(\Phi+\Psi).$$

3.1.6 The Energy-Momentum Tensor

The last step of the EFE derivation is to consider the EMT, T^{μ}_{ν} which act as sources to the Einstein tensor, G^{μ}_{ν}.

For G^0_0, its corresponding source is T^0_0. Based on the definition stated in subsection 1.2, $T^0_0 = -\rho$[26]. Thus, T^0_0 is minus the sum of energy densities of all particles in the universe, whose formula is given by [23]

$$T^0_0(\vec{x}, t) = -\sum_i g_i \int \frac{d^3p}{(2\pi)^3} E_i(p) f_i(\vec{p}, \vec{x}, t), \tag{3.15}$$

where i labels the particle species, g_i is their spin degeneracy, $E_i = \sqrt{p^2 + m_i^2}$ is the energy of a particle with momentum, p and mass m_i. Meanwhile, f_i is the distribution function of the particle species. The particle species considered here are photons, neutrinos, baryons and dark matter. The details of each species is beyond the scope of this dissertation, hence we will only state their relevant contributions to the EMT.

Photons The RHS of equation (3.15) for photons is:

$$T^0_{0\gamma} = -\rho_\gamma[1 + 4\Theta_0].$$

Here, Θ_0 is the perturbations to the photon distribution function integrated over all directions [23].

Neutrinos The contribution from the neutrino species in equation (3.15) is summarised as

$$T^0_{0\nu} = -\rho_\nu[1 + 4\mathcal{N}_0],$$

where $\mathcal{N}_0$ encapsulates perturbations to the neutrino distribution [23].

Baryons and Dark Matter Both baryons and dark matter contribute to the temporal energy-momentum tensor, T^0_{0i} as:

$$T^0_0 = -\rho_i(1 + \delta_i),$$

where i labels baryons, b and dark matter, dm.

Summary Summing all these contributions gives the overall T^0_0 that sources G^0_0 up to first order:

$$T^0_0 = -(\rho_\gamma + \rho_\nu + \rho_b + \rho_{dm}) - (\rho_\gamma 4\Theta_0 + \rho_\nu 4\mathcal{N}_0 + \rho_b\delta_b + \rho_{dm}\delta_{dm}). \tag{3.16}$$

Similarly, T^i_j acts as a source for G^i_j, however, since only the longitudinal, traceless part of G^i_j is extracted, the same must be done for T^i_j:

$$\left(k_i k_j - \frac{\delta_{ij}}{3}\right)(T^i_j) = \sum_i g_i \int \frac{d^3p}{(2\pi)^3} \frac{p^2\mu^2 - (1/3)p^2}{E_i(p)} f_i(\underline{p}). \tag{3.17}$$

Since $\mu^2 - (1/3) = (2/3)\mathcal{P}_2(\mu)$, the integral extracts only the quadruple part of the distribution, which is absent in the zero-order of f_i [23]. Hence, T^i_j is a first-order term contributed only by photons and neutrinos[27],

$$T^i_j = \frac{8}{3}(\rho_\gamma\Theta_0 + \rho_\nu\mathcal{N}_0). \tag{3.18}$$

[26] The minus sign comes from the contraction between g^{00} and T_{00}.

[27] T^i_j is also known as the *anisotropic stress*.

3.1.7 The Scalar-Perturbed Einstein Equation

We end this subsection on scalar perturbations by putting together all the preceding results to finally arrive at the dynamical equations of Ψ and Φ.

The First Evolution Equation of Ψ and Φ

Substituting G_0^0 and T_0^0 in $G_0^0 = 8\pi G_N T_0^0$ gives:

$$-3H^2 + 6\Psi H^2 - 6H\Phi_{,0} - 2\frac{k^2}{a^2}\Phi = -8\pi G_N(\rho_\gamma + \rho_\nu + \rho_b + \rho_{dm} + 4\rho_\gamma\Theta_0 + 4\rho_\nu\mathcal{N}_0 + \rho_b\delta_b + \rho_{dm}\delta_{dm}).$$

The first-order part of this equation gives the first evolution equation of Ψ and Φ:

$$3\Psi H^2 - 3H\Phi_{,0} - \frac{k^2}{a^2}\Phi = -4\pi G_N(4\rho_\gamma\Theta_0 + 4\rho_\nu\mathcal{N}_0 + \rho_b\delta_b + \rho_{dm}\delta_{dm}). \tag{3.19}$$

This equation can be re-expressed in terms of conformal time, η by replacing the dots with apostrophes and adding $\frac{1}{a}$ for each cosmic time derivative that appears in the equation:

$$-3\frac{a'}{a^2}\frac{\Phi'}{a} + 3\Psi\frac{a'^2}{a^4} - \frac{k^2}{a^2}\Phi = -4\pi G_N(4\rho_\gamma\Theta_0 + 4\rho_\nu\mathcal{N}_0 + \rho_b\delta_b + \rho_{dm}\delta_{dm}).$$

Here, $a' = \frac{da}{d\eta}$. Thus, in terms of conformal time, this equation is written as:

$$k^2\Phi + 3\frac{a'}{a}\left(\Phi' - \Psi\frac{a'}{a}\right) = 4\pi G_N a^2(4\rho_\gamma\Theta_0 + 4\rho_\nu\mathcal{N}_0 + \rho_b\delta_b + \rho_{dm}\delta_{dm}). \tag{3.20}$$

The Second Evolution Equation of Ψ and Φ

Since both G_j^i and T_j^i consist of only first-order terms, their substitution into $G_j^i = 8\pi G_N T_j^i$ directly results in the second evolution equation of Ψ and Φ:

$$k^2(\Phi + \Psi) = -32\pi G_N a^2(\rho_\gamma\Theta_0 + \rho_\nu\mathcal{N}_0). \tag{3.21}$$

3.2 Tensor Perturbations

This subsection comprises the derivation of the tensor-perturbed Einstein equations. Built on the intuition developed in the previous scalar perturbation case, the calculations in this subsection are more straightforward.

3.2.1 The Inverse Tensor-Perturbed FRW Metric

Recall the tensor-perturbed FRW metric established in subsubsection 2.2.2. Using the same method as in the case for scalar perturbations, the components of the inverse of this metric are as follows:

$$\begin{aligned} g^{00} &= -1, \\ g^{0i} &= 0, \\ g^{ij} &= \frac{(\delta_{ij} - \mathcal{H}_{ij})}{a^2}, \end{aligned} \tag{3.22}$$

where $\mathcal{H}_{ij}$ is the divergenceless, traceless and symmetric tensor defined in equation (2.7).

3.2.2 Christoffel Symbols

Again, recall the formula for the Christoffel symbol given in equation (1.9) but with $g_{\mu\nu}$ now representing the tensor-perturbed FRW metric:

$$\Gamma^{\alpha}_{\mu\nu} = \frac{1}{2} g^{\alpha\gamma}(g_{\gamma\mu,\nu} + g_{\gamma\nu,\mu} - g_{\mu\nu,\gamma}). \tag{3.23}$$

In **Case 1** where $\alpha = 0$, γ must also equal to zero for the equation to give non-zero values. It transforms into the same form as equation (3.3). This equation is now evaluated for the different values of μ and ν.

Case 1.1 When $\mu = \nu = 0$, only one term in the parentheses survives as the other two cancel each other,

$$\Gamma^{0}_{00} = \frac{1}{2} g^{00}(g_{00,0}).$$

However, since g_{00} has no time-dependence, the overall term becomes zero.

Case 1.2 In this instance, $\mu = 0$ whereas $\nu = i$.

$$\Gamma^{0}_{0i} = \frac{1}{2} g^{00}(g_{00,i} + g_{0i,0} - g_{0i,0}).$$

Again, the overall term equals to zero, as $g_{0i} = 0$ and g_{00} has no spatial-dependence.

Case 1.3 When $\mu = i$ and $\nu = j$, only the third term in the bracket remains, as the first two equal to zero since $g_{0i} = g_{0j} = 0$. It becomes:

$$\Gamma^{0}_{ij} = \frac{1}{2}(-1)(-1) g_{ij,0} = \frac{1}{2}\left[\frac{\partial}{\partial t}(a^2\delta_{ij} + a^2\mathcal{H}_{ij})\right].$$

Performing the time-derivatives gives:

$$\begin{aligned} \frac{\partial}{\partial t}(a^2\delta_{ij}) &= 2\delta_{ij}\dot{a}a, \\ \frac{\partial}{\partial t}(a^2\mathcal{H}_{ij}) &= 2\dot{a}a\mathcal{H}_{ij} + a^2\mathcal{H}_{ij,0}. \end{aligned}$$

By summing the two results, the Christoffel symbol is obtained,

$$\Gamma^0_{ij} = \frac{1}{2}[2\dot{a}a(\delta_{ij} + \mathcal{H}_{ij}) + a^2\mathcal{H}_{ij,0}] = Hg_{ij} + \frac{a^2\mathcal{H}_{ij,0}}{2},$$

where in the second equality, $\dot{a} = Ha$ was substituted, and the spatial component of the tensor-perturbed metric, $g_{ij} = a^2(\delta_{ij} + \mathcal{H}_{ij})$ was used.

In **Case 2** where $\alpha = i$, γ must equal to l for equation (3.23) to give non-zero values. This equation transforms into the same form as equation (3.4). The different cases of μ and ν are now considered.

Case 2.1 When $\mu = \nu = 0$, the three terms in the parentheses equal to zero as $g_{l0} = 0$ and g_{00} has no space-dependence:

$$\Gamma^i_{00} = \frac{1}{2}g^{il}(g_{l0,0} + g_{l0,0} - g_{00,l}) = 0.$$

Case 2.2 For values $\mu = 0$ and $\nu = j$, only the first term remains as the last two are spatial derivatives of $g_{l0} = 0$ and $g_{0j} = 0$:

$$\Gamma^i_{0j} = \frac{g^{il}}{2}g_{lj,0}.$$

Since the time-derivative of g_{ij} was already worked out in **Case 1.3**, the same result can be substituted in this case but with $i = l$,

$$\Gamma^i_{0j} = \frac{g^{il}}{2}(2Hg_{lj} + a^2\mathcal{H}_{lj,0}) = Hg^{il}g_{lj} + \frac{a^2g^{il}\mathcal{H}_{lj,0}}{2}.$$

By utilising the metric property, $g^{il}g_{lj} = \delta_{ij}$ and substituting the spatial component of the inverse tensor-perturbed metric, $g^{il} = \frac{(\delta_{il} - \mathcal{H}_{il})}{a^2}$, the final result of this case is

$$\Gamma^i_{0j} = H\delta_{ij} + \frac{1}{2}\mathcal{H}_{ij,0}.$$

Case 2.3 Lastly, when $\mu = j$ and $\nu = k$, the Christoffel symbol transforms into

$$\Gamma^i_{jk} = \frac{(\delta_{ij} - \mathcal{H}_{ij})}{2a^2}(g_{lj,k} + g_{lk,j} - g_{jk,l}).$$

Similar to **Case 2.3** for the scalar perturbations, it is sufficient to use the example

$$g_{lj,k} = \frac{\partial}{\partial k^k}(a^2\delta_{lj} + a^2\mathcal{H}_{lj}) = a^2\mathrm{i}k_k\mathcal{H}_{lj},$$

and apply the same result to the other terms by exchanging their indices:

$$\Gamma^i_{jk} = \frac{\mathrm{i}}{2}\frac{(\delta_{il} - \mathcal{H}_{il})}{a^2}a^2[k_k\mathcal{H}_{lj} + k_j\mathcal{H}_{lk} - k_l\mathcal{H}_{jk}].$$

After eliminating the delta function outside the parentheses by setting $l = i$, expanding the brackets and neglecting the second-order terms, one would arrive at:

$$\Gamma^i_{jk} = \frac{\mathrm{i}}{2}(k_k\mathcal{H}_{ij} + k_j\mathcal{H}_{ik} - k_i\mathcal{H}_{jk}).$$

Summary To conclude, all the non-zero tensor-perturbed Christoffel symbols up to first-order are:

$$\begin{aligned}\Gamma^0_{ij} &= H g_{ij} + \frac{a^2 \mathcal{H}_{ij,0}}{2}, \\ \Gamma^i_{0j} &= H \delta_{ij} + \frac{1}{2}\mathcal{H}_{ij,0}, \\ \Gamma^i_{jk} &= \frac{\mathrm{i}}{2}(k_k \mathcal{H}_{ij} + k_j \mathcal{H}_{ik} - k_i \mathcal{H}_{jk}).\end{aligned} \tag{3.24}$$

With these values, one can proceed to compute the tensor-perturbed Ricci tensors, $R_{\gamma\nu}$ in the next subsubsection.

3.2.3 Ricci Tensors

This subsubsection focuses on computing the tensor-perturbed Ricci tensors, $R_{\gamma\nu}$. As before, only the temporal and spatial Ricci tensors are considered.

Case 1 For $\gamma = \nu = 0$, the Ricci tensor formula takes a form identical to equation (3.7). However, since both Γ^0_{00} and Γ^i_{00} are zero, only the second and fourth terms survive,

$$R_{00} = -\Gamma^{\alpha}_{0\alpha,0} - \Gamma^{\alpha}_{\beta 0}\Gamma^{\beta}_{0\alpha}.$$

The next step is to consider the different values of α and β.

Case 1.1 This case considers the value $\alpha = 0$,

$$R_{00} = -\Gamma^0_{00,0} - \Gamma^0_{\beta 0}\Gamma^{\beta}_{00} = 0.$$

The overall term becomes zero as all the Christoffel symbols that make up this term are equal to zero.

Case 1.2 Next, consider the case where $\alpha = i$:

$$R_{00} = -\Gamma^i_{0i,0} - \Gamma^0_{\beta 0}\Gamma^{\beta}_{00}.$$

For non-zero values, we must set $\beta = j$.

The first term,

$$-\Gamma^i_{0i,0} = -\frac{\partial}{\partial t}\left[H\delta_{ii} + \frac{1}{2}\mathcal{H}_{ii,0}\right] = -3\frac{\ddot{a}}{a} + 3H^2 - \frac{\mathcal{H}_{ii,0}}{2},$$

is simplified further by noting that $\mathcal{H}_{ii,0} = 0$ since H_{ij} is traceless.

The second term,

$$-\Gamma^i_{j0}\Gamma^j_{0i} = -\left[(H\delta_{ij} + \frac{1}{2}\mathcal{H}_{ij,0})(H\delta_{ji} + \frac{1}{2}\mathcal{H}_{ji,0})\right],$$

only contains one first-order term as the product of $\mathcal{H}_{ij}$ and δ_{ij} results in a second-order term. Expanding the brackets gives:

$$-\Gamma^i_{j0}\Gamma^j_{0i} = -\left[H^2\delta_{ij}\delta_{ji} + \frac{1}{2}H\delta_{ij}\mathcal{H}_{ji,0} + \frac{1}{2}H\delta_{ij}\mathcal{H}_{ji,0} + \frac{1}{4}\mathcal{H}_{ij,0}\mathcal{H}_{ji,0}\right].$$

The last three terms are at second-order and thus, neglected. The delta functions in the remaining term are eliminated by first setting $j = i$ and then noting that $\delta_{ii} = 3$.

Summary Summing these results gives:

$$R_{00} = -3\frac{\ddot{a}}{a} + 3H^2 - 3H^2 = -3\frac{\ddot{a}}{a} \tag{3.25}$$

The expression is identical to the temporal Ricci tensor obtained in the derivation of the Friedmann equations, which means that at first order, it is not affected by tensor perturbations. Consequently, its corresponding Einstein equation is unaffected, either [23].

Case 2 When $\gamma = i$ and $\nu = j$, the formula is similar to that of equation (3.9). Now, we can break the derivation into three parts.

Part 1 The first step is to consider the first two terms and expand them by their α values:

$$\Gamma^{\alpha}_{ij,\alpha} - \Gamma^{\alpha}_{i\alpha,j} = \Gamma^{0}_{ij,0} - \Gamma^{0}_{i0,j} + \Gamma^{k}_{ij,k} - \Gamma^{k}_{ik,j}.$$

We can ignore the second term since $\Gamma^{0}_{i0} = 0$, as well as the fourth term since

$$\Gamma^{k}_{ik} = \frac{\mathrm{i}}{2}(k_k \mathcal{H}_{ki} + k_i \mathcal{H}_{kk} - k_k \mathcal{H}_{ik}) = k_i \mathcal{H}_{kk} = 0,$$

due to $\mathcal{H}_{ij}$ being traceless.

From the calculation in **Case 1.3** of subsubsection 3.2.2, we know that $\Gamma^{0}_{ij} = \frac{g_{ij,0}}{2}$. Hence, the first term, $\Gamma^{0}_{ij,0}$ is $\frac{g_{ij,00}}{2}$. By working out the second-oder time derivative, we have:

$$\begin{aligned}
\Gamma^{0}_{ij,0} &= \frac{1}{2}\frac{d}{dt}\left[\frac{d}{dt}\{a^2(\delta_{ij} + \mathcal{H}_{ij})\}\right] \\
&= \frac{1}{2}\frac{d}{dt}[2\dot{a}a\delta_{ij} + 2\dot{a}a\mathcal{H}_{ij} + a^2\mathcal{H}_{ij,0}] \\
&= \frac{1}{2}[2\ddot{a}a(\delta_{ij} + \mathcal{H}_{ij}) + 2\dot{a}^2(\delta_{ij} + \mathcal{H}_{ij}) + 4\dot{a}a\mathcal{H}_{ij,0} + a^2\mathcal{H}_{ij,00}].
\end{aligned}$$

By substituting the relation $g_{ij} = a^2(\delta_{ij} + \mathcal{H}_{ij})$ into the first two terms, this result becomes:

$$\Gamma^{0}_{ij,0} = g_{ij}\left(\frac{\dot{a}}{a} + H^2\right) + 2a^2 H\mathcal{H}_{ij,0} + \frac{a^2\mathcal{H}_{ij,00}}{2}. \tag{3.26}$$

Next, the third term, $\Gamma^{k}_{ij,k}$ is just the spatial derivative of Γ^{k}_{ij} with respect to k^k. Its result is given by

$$\Gamma^{k}_{ij,k} = \frac{1}{2}[-k_i k_j \mathcal{H}_{jk} - k_j k_k \mathcal{H}_{ik} + k_k k_k \mathcal{H}_{ji}] = \frac{k^2}{2}\mathcal{H}_{ij}, \tag{3.27}$$

where in the last equality, recall that the wavevector, $\vec{k}$ points in the z-direction, and so it imposes that $i = j = 3$, which leads to $\mathcal{H}_{jk} = \mathcal{H}_{3k}$ and $\mathcal{H}_{ik} = \mathcal{H}_{3k}$ to be zero. Hence, the result of **Part 1** is just the sum of results (3.26) and (3.27).

Part 2 Next, we look at the third term in R_{ij}, which is $-\Gamma^{\alpha}_{\alpha\beta}\Gamma^{\beta}_{ij}$. We expand this term twice,

$$\begin{aligned}
-\Gamma^{\alpha}_{\alpha\beta}\Gamma^{\beta}_{ij} &= -\Gamma^{0}_{0\beta}\Gamma^{\beta}_{ij} - \Gamma^{k}_{k\beta}\Gamma^{\beta}_{ij} \\
&= -\Gamma^{0}_{00}\Gamma^{0}_{ij} - \Gamma^{0}_{0l}\Gamma^{l}_{ij} - \Gamma^{k}_{k0}\Gamma^{0}_{ij} - \Gamma^{k}_{kl}\Gamma^{l}_{ij},
\end{aligned}$$

such that in the first line, it is expanded for values $\alpha = 0, k$ and in the second line, the first line is further expanded in terms of $\beta = 0$ and $\beta = l$. The first and second terms are zero, as they consist of Christoffel symbols which are equivalent to zero, whereas the fourth term is negligible since it would result in second-order terms. Thus, we only need to work out the third term.

Recalling the non-zero Christoffel symbols in equation (3.23), this term is given by:

$$-\Gamma^k_{k0}\Gamma^0_{ij} = \left[H\delta_{kk} + \frac{\mathcal{H}_{kk,0}}{2}\right]\left[Hg_{ij} + \frac{a^2\mathcal{H}_{ij,0}}{2}\right].$$

The first square bracket reduces to $3H$ since the sum over k results in $\delta_{kk} = 3$ and $\mathcal{H}_{kk} = 0$. Meanwhile, based on **Case 1.3** in subsubsection 3.2.2, the terms in the second square bracket are equivalent to $\frac{g_{ij,0}}{2}$. Thus, multiplying the two gives

$$-\Gamma^k_{k0}\Gamma^0_{ij} = \frac{3}{2}Hg_{ij,0}.$$

Part 3 The last term in R_{ij} to consider is $-\Gamma^\alpha_{\beta j}\Gamma^\beta_{i\alpha}$. Expanding it in terms of its α and β values gives

$$-\Gamma^\alpha_{\beta j}\Gamma^\beta_{i\alpha} = -\Gamma^0_{0j}\Gamma^0_{i0} - \Gamma^0_{lj}\Gamma^l_{i0} - \Gamma^k_{0j}\Gamma^0_{ik} - \Gamma^k_{lj}\Gamma^l_{ik}.$$

As in **Part 2**, the first term is zero since its Christoffel symbols are zero, whereas the fourth term is trivial as it results in second-order terms. By inspection, the second and third terms have a similar form, hence they are rewritten as a sum of two identical terms after relabelling their indices:

$$-2\Gamma^0_{kj}\Gamma^k_{i0} = -\delta_{ik}Hg_{kj,0} - g_{kj,0}\mathcal{H}_{ik,0}.$$

Again, recall that $g_{kj,0} = 2Hg_{kj} + a^2\mathcal{H}_{kj,0}$ from subsubsection 3.2.2. By substituting this into the equation and neglecting the second-order terms, we have

$$-2\Gamma^0_{kj}\Gamma^k_{i0} = -2\delta_{ik}H^2g_{kj} - 2Hg_{kj}\mathcal{H}_{ik,0} = -2H^2g_{ij} - 2a^2H\mathcal{H}_{ij,0},$$

where in the last equality, we set $k = i$ in the first term and substituted g_{kj} into the second term. The result is only considered up to first-order.

Summary Thus, by summing the results of **Part 1**, **Part 2** and **Part 3**, we have the tensor-perturbed spatial Ricci tensor:

$$R_{ij} = g_{ij}\left(\frac{\ddot{a}}{a} + 2H^2\right) + \frac{3}{2}a^2H\mathcal{H}_{ij,0} + \frac{a^2}{a}\mathcal{H}_{ij,00} + \frac{k^2}{2}\mathcal{H}_{ij}. \tag{3.28}$$

3.2.4 Ricci Scalar

Similar to the scalar perturbation case, the computation of the Ricci scalar using the tensor-perturbed Ricci tensors is divided into two parts.

Part 1

$$g^{00}R_{00} = (-1)\left[-3\frac{\ddot{a}}{a}\right] = 3\frac{\ddot{a}}{a}$$

Part 2

$$g^{ij}R_{ij} = g^{ij}\left[g_{ij}\frac{\ddot{a}}{a} + 2g_{ij}H^2 + \frac{3}{2}a^2H\mathcal{H}_{ij,0} + \frac{a^2}{a}\mathcal{H}_{ij,00} + \frac{k^2}{2}\mathcal{H}_{ij}\right]$$

By multiplying g^{ij} with all the terms in the square bracket, $g^{ij}R_{ij}$ consists of the terms:

$$g^{ij}g_{ij}\frac{\ddot{a}}{a} + 2g^{ij}g_{ij}H^2 + \frac{3}{2}a^2Hg^{ij}\mathcal{H}_{ij,0} + \frac{a^2}{a}g^{ij}\mathcal{H}_{ij,00} + \frac{k^2}{2}g^{ij}\mathcal{H}_{ij}.$$

After substituting the relation $a^2g^{ij} = (\delta_{ij} - \mathcal{H}_{ij})$ and neglecting all second-order terms, we have the result,

$$g^{ij}R_{ij} = 3\left(\frac{\ddot{a}}{a} + 2H^2\right),$$

where the factor of 3 comes from the contraction of $g^{ij}g_{ij}$.

Summing the two parts gives the tensor-perturbed Ricci scalar, $\mathcal{R}$:

$$\mathcal{R} = 6\left(\frac{\ddot{a}}{a} + H^2\right). \tag{3.29}$$

By comparing this result to equation (1.13), we deduce that $\delta\mathcal{R} = 0$. While R_{ij} does contain tensor perturbations (unlike its temporal counterpart), these perturbations have no contribution in the final Ricci scalar.

3.2.5 The Einstein Tensor

As seen in the precedent subsubsections, the Ricci scalar, $\mathcal{R}$ and the temporal Ricci tensor, R_{00} have no contributions from the tensor perturbations, which are only found in the spatial Ricci tensor, R_{ij}. This means that only the spatial Einstein tensor, G^i_j is affected by the tensor perturbations. Therefore, we can immediately dive into the computation of its first-order part, δG^i_j for interesting results. Since $\delta\mathcal{R} = 0$, δG^i_j is just δR^i_j.

To get δR^i_j we must first perform the contraction, $g^{ik}R_{kj}$. This gives the zero and first-order parts of R^i_j:

$$R^i_j = \delta^i_j\left(\frac{\dot{a}}{a} + 2H^2\right) + \frac{3}{2}a^2 g^{ik}H\mathcal{H}_{kj,0} + \frac{a^2}{2}g^{ik}\mathcal{H}_{jk,00} + \frac{k^2}{2}g^{ik}\mathcal{H}_{kj}.$$

By using the same g^{ik} substitution as in the previous calculations demonstrated in this subsection and neglecting the second-order terms, we arrive at:

$$\delta R^i_j = \frac{3}{2}\delta_{ik}H\mathcal{H}_{kj,0} + \frac{1}{2}\delta_{ik}\mathcal{H}_{jk,00} + \frac{1}{2}\frac{k^2}{a^2}\delta_{ik}\mathcal{H}_{jk}, \tag{3.30}$$

which is equivalent to δG^i_j.

3.2.6 The Energy-Momentum Tensor

As a continuation to subsubsection 3.2.5, only the spatial first-order EMT, δT^i_j will be considered here. Similarly to the scalar perturbation case, this is given by the anisotropies generated by the tensor perturbations [23].

Tensor perturbations induced by h_+ lead to anisotropies in the form of

$$\Theta(\mu,\phi) = (1-\mu^2)\cos(2\phi)\Theta_+(\mu),$$

and those induced by $h_\times$ take the form,

$$\Theta(\mu,\phi) = (1-\mu^2)\sin(2\phi)\Theta_\times(\mu).$$

However, we can approximate these anisotropies to zero in our calculations since their contributions to the overall evolution of h_+ and $h_\times$ are very trivial. Physically, this means that the tensor perturbations have no source.

3.2.7 The Tensor-Perturbed Einstein Equations

This subsection on tensor perturbations is concluded by combining all preceding results to finally arrive at the dynamical equations of h_+ and $h_\times$. From equation (3.30), δG^i_j is proportional to $\mathcal{H}_{ij}$ as well as its derivatives. Therefore, to find the equations for h_+ and $h_\times$ separately, one needs to consider their respective positions in $\mathcal{H}_{ij}$.

The Evolution Equation of h_+

Note that in $\mathcal{H}_{ij}$, h_+ is labelled as $\mathcal{H}_{11}$ and $-\mathcal{H}_{22}$. Using this definition of h_+, it is straightforward to see that $\delta G^1_1 = -\delta G^2_2$. Hence,

$$\begin{aligned}\delta G^1_1 - \delta G^2_2 &= \frac{3}{2}H\mathcal{H}_{11,0} + \frac{1}{2}\mathcal{H}_{11,00} + \frac{1}{2}\frac{k^2}{a^2}\mathcal{H}_{11} + \frac{3}{2}H\mathcal{H}_{11,0} + \frac{1}{2}\mathcal{H}_{11,00} + \frac{1}{2}\frac{k^2}{a^2}\mathcal{H}_{11},\\ &= 3Hh_{+,0} + h_{+,00} + \frac{k^2}{a^2}h_+,\end{aligned}$$

where in the last line, we reinstated h_+. Since $\delta T^1_1 = \delta T^2_2 = 0$, the evolution equation for h_+ is just

$$\ddot{h}_+ + 3H\dot{h}_+ + \frac{k^2}{a^2}h_+ = 0. \tag{3.31}$$

This can be re-expressed in terms of conformal time, η as

$$h''_+ + 2\frac{a'}{a}h'_+ + k^2h_+ = 0, \tag{3.32}$$

where the factor of a^2 on the LHS is cancelled off by dividing the entire equation by a^2.

The Evolution Equation of $h_\times$

On the other hand, $h_\times = \mathcal{H}_{12} = \mathcal{H}_{21}$, thus calculating $\delta G^1_2 + \delta G^2_1$ and noting that $\delta T^1_2 = \delta T^2_1 = 0$ leads to an identical evolution equation but with h_+ now replaced with $h_\times$:

$$\ddot{h}_\times + 3H\dot{h}_\times + \frac{k^2}{a^2}h_\times = 0, \tag{3.33}$$

which, in terms of conformal time, η is written as:

$$h''_\times + 2\frac{a'}{a}h'_\times + k^2h_\times = 0. \tag{3.34}$$

Summary Generalising equations (3.32) and (3.34) gives:

$$h''_\alpha + 2\frac{a'}{a}h'_\alpha + k^2h_\alpha = 0, \tag{3.35}$$

where $\alpha = +, \times$. By inspection, this is a wave equation whose solutions are the PGWs we have introduced in subsubsection 1.1.2. In fact, the form of this equation reaffirms $\mathcal{H}_{ij}$ as a tensor representing the PGWs. Since inflation predicts these PGWs, their detection is crucial in solidifying the theory as a standard cosmological model.

3.3 Proving the Decomposition Theorem

Previously, we assumed the notion that scalar and tensor perturbations in the metric evolve independently. Now that we have the perturbed Einstein equations, we can prove that the decomposition theorem is indeed obeyed. The steps of the proof follow that of Chapter 5 in *Modern Cosmology* by Dodelson, 2003 [23].

The proof itself is rather short and uses deductive reasoning. Since the evolution equations of Ψ and Φ are obtained from the scalar-perturbed temporal Einstein tensor, G^0_0 and the longitudinal, traceless part of its corresponding spatial component, $\left(k_i k_j - \frac{\delta_{ij}}{3}\right) G^i_j$, we can deduce that the theorem is true if we show the absence of tensor perturbations in these components [23]. We already know from subsubsection 3.2.5 that tensor perturbations are absent in G^0_0, hence we need only analyse the longitudinal, traceless part of the tensor-perturbed spatial Einstein tensor, δG^i_j:

$$\left(k_i k_j - \frac{\delta_{ij}}{3}\right) \delta G^i_j = \left(k_i k_j - \frac{\delta_{ij}}{3}\right) \times \left[\frac{3}{2}\delta_{ik} H \mathcal{H}_{kj,0} + \frac{1}{2}\delta_{ik}\mathcal{H}_{jk,00} + \frac{1}{2}\frac{k^2}{a^2}\delta_{ik}\mathcal{H}_{jk}\right].$$

Since all terms in δG^i_j is proportional to δ_{ij}, when acted on by the projection operator, the result is null - as predicted by the decomposition theorem. This also indirectly reaffirms GWs to be transverse. Therefore, sources that induce scalar perturbations do not induce tensor perturbations. Moreover, the fact that the anisotropic stress is only contributed by scalar perturbations (since we have seen that it goes to zero for tensor perturbations in subsubsection 3.2.6), is another manifestation of this theorem.

4 The Perturbation Power Spectra

Following the derivation of the evolution equations of the metric perturbations and understanding their physical interpretation, our treatment of these perturbations will only be complete by accounting for their quantum nature. Thus, this section aims to quantise the perturbations and consequently derive their power spectra, spectral indices and the consistency condition of a single-field inflation model. By the end of the section, the significance of these quantities in observational work is discussed.

4.1 Quantum-Mechanical Approach

Assuming a classical origin of the primordial inhomogeneities results in a contradiction to the perturbative approach taken in equation (2.1). In a classical picture, the inflationary period (which constitutes a minimum of 60 e-folds) dictates energy density fluctuations larger than its homogeneous background [42]. Thus, violation of perturbation theory by classical fluctuations necessitates a quantum-mechanical approach as not only are vacuum quantum fluctuations unaffected by inflation, but they also possess the Gaussian statistics found in the CMB [45, 55, 56]. The process starts with quantising the action of the inflation scalar field[28], (1.18) as seen in various literature [14, 42, 43, 47, 58, 65, 69]. The derivation in this dissertation closely follows the concise working in [69], whose simplified form is adequate given the framework set up in our preceding sections.

4.1.1 The Reduced Planck Mass

Before quantising our perturbations, it is useful to introduce the *reduced Planck mass*[29], $M_{Pl} = \frac{1}{\sqrt{8\pi G_N}}$ and rewrite our Friedmann equations, (1.14) and (1.15) in terms of this quantity [69]:

$$\begin{aligned} H^2 &= \frac{1}{3M_{Pl}^2}\rho, \\ \dot{H} + H^2 &= -\frac{1}{6M_{Pl}^2}(\rho + 3P). \end{aligned} \tag{4.1}$$

We can also re-express the slow-roll parameters in equations (1.23) and (1.24) as:

$$\begin{aligned} \epsilon \equiv \frac{1}{2M_{Pl}^2}\frac{\dot{\varphi}^2}{H^2} \approx \epsilon_V \equiv \frac{M_{Pl}^2}{2}\left(\frac{V_{,\varphi}}{V}\right)^2, \\ \tau \approx 4\epsilon_V - 2\tau_V, \end{aligned} \tag{4.2}$$

where $\tau_V \equiv M_{Pl}^2 \frac{V_{,\varphi\varphi}}{V}$. ϵ_V and τ_V are the *potential slow-roll parameters*[30].

[28] An alternate approach involves redefining the perturbations and directly modifying the evolution equations such that the perturbations behave like simple harmonic oscillators, quantising them and inferring their power spectra from their quantum variance [23].

[29] The *Planck mass* refers to mass in Planck units, $m_{Pl} = \sqrt{\frac{\hbar c}{G_N}}$ where $\hbar = c = 1$. Dividing this quantity by $\sqrt{8\pi}$ gives the reduced Planck mass.

[30] We can also rewrite the slow-roll parameters in terms of the Hubble rate, H. Thus, they are called the *Hubble slow-roll prameters*.

4.1.2 Quantising Inflation

Recall the action of inflation (1.18) in its explicit form using conformal time, η:

$$\mathcal{S} = \int \frac{1}{2} a^2 [\varphi'^2 - (\nabla\varphi)^2 - 2a^2 V(\varphi)] \, \mathrm{d}\eta \mathrm{d}^3\mathrm{x}. \tag{4.3}$$

Next, we replace φ with the redefined field, $f(\eta, \vec{x}) = a(\eta)\delta\varphi(\eta, \vec{x})$ and expand the action up to second order whilst neglecting the metric perturbations:

$$\begin{aligned}
\mathcal{S}^{(2)} &= \frac{1}{2}\int a^2 \left[\left(\frac{f'}{a} - \frac{\mathbf{H}f}{a} \right)^2 - \left(\frac{\nabla f}{a} \right)^2 - a^2 V_{,\varphi\varphi} \left(\frac{f}{a} \right)^2 \right] \mathrm{d}\eta \mathrm{d}^3\mathrm{x} \\
&= \frac{1}{2}\int [f'^2 - (\nabla f)^2 - \mathbf{H}(f^2)' + (\mathbf{H}^2 - a^2 V_{,\varphi\varphi}) f^2] \, \mathrm{d}\eta \mathrm{d}^3\mathrm{x} \\
&= \frac{1}{2}\int [f'^2 - (\nabla f)^2 + (\mathbf{H}' + \mathbf{H}^2 - a^2 V_{,\varphi\varphi}) f^2] \, \mathrm{d}\eta \mathrm{d}^3\mathrm{x} \\
&= \frac{1}{2}\int \left[f'^2 - (\nabla f)^2 + \left(\frac{a''}{a} - a^2 V_{,\varphi\varphi} \right) \right] \mathrm{d}\eta \mathrm{d}^3\mathrm{x},
\end{aligned}$$

where the subscript (2) indicates up to second order. We also denoted the comoving Hubble radius as $\mathbf{H} = \frac{1}{aH}$ to avoid cluttering[31]. Furthermore, here $V_{,\varphi\varphi} = \frac{\partial^2 V}{\partial(\varphi^{(0)})^2}$ and ∇ is the gradient operator. From our slow-roll approximations in subsubsections 1.2.4 and 1.2.5, the first Friedmann equation in (4.1) gives:

$$\frac{a''}{a} \approx 2a^2 H^2 \approx \frac{2}{3\tau_V} a^2 V_{,\varphi\varphi} >> a^2 V_{,\varphi\varphi},$$

where we used a constant H, $\rho \approx V$ and $\tau << 1$ [69]. This leads to the final result of the second-order action,

$$\mathcal{S}^{(2)} = \int \frac{1}{2} \left[f'^2 - (\nabla f)^2 + \frac{a''}{a} f^2 \right] \mathrm{d}\eta \mathrm{d}^3\mathrm{x}, \tag{4.4}$$

from which the following Lagrangian, $\mathcal{L}$ can be extracted [69]:

$$\mathcal{L} = \frac{1}{2} \left[f'^2 - (\nabla f)^2 + \frac{a''}{a} f^2 \right]. \tag{4.5}$$

The Euler-Lagrange equation corresponding to $\mathcal{L}$ is the *Mukhanov-Sasaki equation*, written as:

$$f'' - \nabla^2 f - \frac{a''}{a} f^2 = 0. \tag{4.6}$$

To quantise $f(\eta, \vec{x})$, we apply the *second quantisation* method where we promote it as an operator, $\hat{f}(\eta, \vec{x})$. The same is done to its *conjugate momentum*, $\hat{\pi}(\eta, \vec{x})$ where $\pi(\eta, \vec{x}) = \frac{\partial \mathcal{L}}{\partial f'} \equiv f'$. The two operators obey the *equal-time commutation relations* (ETCR):

$$\begin{aligned}
&[\hat{f}(\eta, \vec{x}), \hat{f}(\eta, \vec{y})] = 0, \\
&[\hat{\pi}(\eta, \vec{x}), \hat{\pi}(\eta, \vec{y})] = 0, \\
&[\hat{f}(\eta, \vec{x}), \hat{\pi}(\eta, \vec{y})] = i\delta(\vec{x} - \vec{y}).
\end{aligned} \tag{4.7}$$

[31] This notation is only introduced now to avoid confusion with the Hubble rate, H in previous sections.

In Fourier space, $\hat{f}(\eta,\vec{x})$ and $\hat{\pi}(\eta,\vec{y})$[32] are written in terms of the time-independent creation operator, $\hat{a}_{\vec{k}}$ and annihilation operator, $\hat{a}^{\dagger}_{\vec{k}}$,

$$\begin{aligned}\hat{f}(\eta,\vec{x}) &= \int \frac{\mathrm{d}^3\mathrm{k}}{(2\pi)^{3/2}}\,(f^*_k\hat{a}^{\dagger}_{\vec{k}}e^{-i\vec{k}\cdot\vec{x}} + f_k\hat{a}_{\vec{k}}e^{i\vec{k}\cdot\vec{x}}),\\ \hat{\pi}(\eta,\vec{y}) &= \int \frac{\mathrm{d}^3\mathrm{k}}{(2\pi)^{3/2}}\,(f'^*_k\hat{a}^{\dagger}_{\vec{k}}e^{-i\vec{k}\cdot\vec{x}} + f'_k\hat{a}_{\vec{k}}e^{i\vec{k}\cdot\vec{x}}),\end{aligned} \tag{4.8}$$

which satisfy:

$$\begin{aligned}\left[\hat{a}_{\vec{k}},\hat{a}_{\vec{k'}}\right] &= 0,\\ \left[\hat{a}^{\dagger}_{\vec{k}},\hat{a}^{\dagger}_{\vec{k'}}\right] &= 0,\\ \left[\hat{a}_{\vec{k}},\hat{a}^{\dagger}_{\vec{k'}}\right] &= \delta(\vec{k}-\vec{k'}).\end{aligned} \tag{4.9}$$

In (4.8), f_k is the solution to the Mukhanov-Sasaki equation in Fourier space,

$$f''_k + \omega^2_k(\eta)f_k = 0, \tag{4.10}$$

where $\omega^2_k(\eta) = k^2 - \frac{a''}{a} \equiv |\vec{k}|$. Recalling our definition of conformal time, η given a constant H in (1.16), $\omega^2_k(\eta) = k^2 - \frac{2}{\eta^2}$, thus the exact solution to equation (4.10) is:

$$f_k(\eta) = A\frac{e^{-ik\eta}}{\sqrt{2k}}\left(1-\frac{i}{k\eta}\right) + B\frac{e^{ik\eta}}{\sqrt{2k}}\left(1+\frac{i}{k\eta}\right).$$

However, since the ETCR, (4.7) and operator relations (4.9) dictate that the Wronskian be

$$\mathcal{W}(f^*_k,f_k) \equiv f^*_k f'_k - f_k f^{*'}_k = -i, \tag{4.11}$$

we can neglect the second term and conclude the solution to be

$$f_k(\eta) = A\frac{e^{-ik\eta}}{\sqrt{2k}}\left(1-\frac{i}{k\eta}\right). \tag{4.12}$$

Moreover, this simplification fulfils the condition $\hat{a}_k|0\rangle = 0$, ie. the vacuum state of a quantum system is the ground state of the Hamiltonian [14].

4.1.3 Power Spectrum of Inflation

With these machinery, we can finally formulate the *power spectrum*, $\mathcal{P}_q$ for a general observable, q via the *quantum variance*,

$$\langle q(\vec{k})q^*(\vec{k'})\rangle \equiv \frac{2\pi^2}{k^3}\mathcal{P}_q(k)\delta(\vec{k}-\vec{k'}). \tag{4.13}$$

By substituting $\hat{f}(\eta,\vec{x})$ and its complex conjugate $\hat{f}^{\dagger}(\eta,\vec{y})$ at $\vec{x}=\vec{y}=0$, we obtain the zero-point fluctuation,

$$\begin{aligned}\langle 0|\hat{f}(\eta,0)\hat{f}^{\dagger}(\eta,0)|0\rangle &= \int \frac{\mathrm{d}^3\mathrm{k}}{(2\pi)^{3/2}}\frac{\mathrm{d}^3\mathrm{k}'}{(2\pi)^{3/2}}f_k f^*_k\langle 0|[\hat{a}_{\vec{k}},\hat{a}^{\dagger}_{\vec{k'}}]|0\rangle\\ &= \int \mathrm{d}\ln\mathrm{k}\,\frac{k^3}{2\pi^2}|f_k|^2.\end{aligned}$$

[32]The use of $\vec{y}$ for $\hat{\pi}$ is a deliberate choice and is perfectly acceptable as it has no effect on the ETCR.

Using (4.13), we can extract the power spectrum of f_k to be $\mathcal{P}_f = \frac{k^3}{2\pi^2}|f_k|^2$. From the definition of $f(\eta, \vec{x})$ in subsubsection 4.1.2, we have the relation $\mathcal{P}_{\delta\varphi} = a^{-2}\mathcal{P}_f$, thus the power spectrum of inflation is

$$\begin{aligned}\mathcal{P}_{\delta\varphi}(k) &= (-H\eta)^2 \frac{k^3}{2\pi^2}\frac{1}{2k}\left[1 + \frac{1}{(k\eta)^2}\right] \\ &= \left(\frac{H}{2\pi}\right)^2 \left(1 + \frac{k^2}{a^2H^2}\right).\end{aligned} \tag{4.14}$$

At *super-horizon scales*[33] where $k\eta >> 1$, it is obvious that $\mathcal{P}_{\delta\varphi}(k) \to \left(\frac{H}{2\pi}\right)^2$. Nonetheless, since the Hubble rate, H varies so slowly in the slow-roll approximation model, we can assume the power spectrum, $\mathcal{P}_{\delta\varphi}(k)$ takes a similar form but with $H = \frac{k}{a} \equiv H_k$ at *horizon crossing*, when $k\eta = 1$ [69].

4.1.4 Power Spectrum of Curvature Perturbations

In determining the power spectrum of the scalar perturbations, it is best to use the *comoving curvature perturbation*, $\mathfrak{R}$, as it is gauge-invariant, unlike the *curvature perturbation*, Ψ. The two quantities are related via:

$$\mathfrak{R} = \Psi + H\frac{\delta\varphi}{\dot{\varphi}^{(0)}}.$$

$\mathfrak{R}$ received its name from the fact that on comoving hypersurfaces[34] where $\delta\varphi = 0$, $\mathfrak{R} = \Psi$ [60]. In observations, $\mathfrak{R}$ is a crucial parameter as it remains constant well after it leaves the horizon for all scales [65], thus it encodes information regarding inflation. Furthermore, since Ψ grows after inflation, it is preferable to probe the power spectrum of the scalar perturbations through $\mathfrak{R}$. Thus, measurement of its spectrum will hope to give the curvature perturbation amplitude of different modes of scales re-entering the horizon during the matter-dominated epoch [65], as mentioned in subsubsection 1.2.3.

For our calculation, it is useful to adopt its definition in the spatially-flat gauge [69],

$$\mathfrak{R} = -H\frac{\delta\varphi}{\dot{\varphi}^{(0)}}, \tag{4.15}$$

as we can easily relate it to $\delta\varphi$ to obtain its power spectrum:

$$\mathcal{P}_{\mathfrak{R}}(k) = \frac{1}{2M_{Pl}^2\epsilon}\left(\frac{k}{2\pi a}\right)^2. \tag{4.16}$$

In addition to this, the *scalar spectral index*, n_s characterises the variation of energy densities with respect to the scale. It is defined as:

$$n_s = 1 + \frac{\mathrm{d}\ln\mathcal{P}_{\mathfrak{R}}(k)}{\mathrm{d}\ln\mathrm{k}}. \tag{4.17}$$

Thus, using this quantity, we can build an approximate power law for the power spectrum of the curvature perturbation,

$$\mathcal{P}_{\mathfrak{R}}(k) = A_s(k_*)\left(\frac{k}{k_*}\right)^{n_s-1}, \tag{4.18}$$

where k_* is denoted as a reference scale.

[33] Contrarily, *sub-horizon scales* refer to $k\eta << 1$.

[34] A hypersurface refers to an $(\mathrm{n}-1)$-dimensional surface which is embedded in an n-dimensional space.

4.1.5 Power Spectrum of Tensor Perturbations

The first step in deriving the power spectrum for the tensor perturbations is to express $\mathcal{H}_{ij}$ in terms of its Fourier modes:

$$\mathcal{H}_{ij} = \sum_{\alpha=+,\times} \int \frac{\mathrm{d}^3\mathrm{k}}{(2\pi)^{2/3}} \mathcal{H}_{ij}^{(\alpha)}(\eta, \vec{k}) e^{i\vec{k}\cdot\vec{x}}, \tag{4.19}$$

where $\mathcal{H}_{ij}^{(\alpha)}(\eta, \vec{k})$ represents the components of $\mathcal{H}_{ij}$ and is written as:

$$\mathcal{H}_{ij}^{(\alpha)}(\eta, \vec{k}) = \frac{1}{\sqrt{2}} m_{ij}^{(\alpha)}(\hat{\vec{k}}) h^{(\alpha)}(\eta, \vec{k}). \tag{4.20}$$

Here, $m_{ij}^{(\alpha)}$ comes from the set of basis tensors,

$$m^{(\alpha)}(\hat{\vec{z}}) = \frac{1}{2}(\hat{\vec{x}} \pm i\hat{\vec{y}}) \otimes (\hat{\vec{x}} \pm i\hat{\vec{y}}) \tag{4.21}$$

that satisfy the orthogonality and reality conditions [69]:

$$\begin{aligned} m_{ij}^{(\alpha)}(\hat{\vec{k}})[m^{(\beta)ij}(\hat{\vec{k}})]^* &= \delta^{\alpha\beta} \\ [m_{ij}^{(\alpha)}(\hat{\vec{k}})]^* = m_{ij}^{(-\alpha)}(\hat{\vec{k}}) &= m_{ij}^{(\alpha)}(-\hat{\vec{k}}). \end{aligned} \tag{4.22}$$

By expanding the summed Einstien-Hilbert and matter action up to second order, we have the second-order action associated to the tensor perturbations [69]:

$$\mathcal{S}^{(2)} = \frac{M_{Pl}^2}{8} \int a^2 (\mathcal{H}'_{ij}\mathcal{H}'^{ij} - \partial_i \mathcal{H}_{jk} \partial^i \mathcal{H}^{jk}) \, \mathrm{d}\eta \mathrm{d}^3\mathrm{x}. \tag{4.23}$$

By incorporating equations (4.19), (4.20) and (4.22) into $S^{(2)}$, we can express its first term as

$$\begin{aligned} \int \mathcal{H}'_{ij}\mathcal{H}'^{ij} \, \mathrm{d}^3\mathrm{x} &= \sum_{\alpha,\beta=+,\times} \int \frac{\mathrm{d}^3\mathrm{k}}{(2\pi)^{2/3}} \frac{\mathrm{d}^3\mathrm{k}'}{(2\pi)^{2/3}} \frac{1}{2} h'^{(\alpha)}(\eta, \vec{k}) h'^{(\beta)}(\eta, \vec{k}') m_{ij}^{(\alpha)}(\hat{\vec{k}}) m^{(\beta)ij}(\hat{\vec{k}'}) \int \mathrm{d}^3\mathrm{x} e^{i(\vec{k}+\vec{k}')\cdot x} \\ &= \frac{1}{2} \sum_{\alpha,\beta=+,\times} \int \frac{\mathrm{d}^3\mathrm{k}}{(2\pi)^{2/3}} \frac{\mathrm{d}^3\mathrm{k}'}{(2\pi)^{2/3}} \, h'^{(\alpha)}(\eta, \vec{k}) h'^{(\beta)}(\eta, \vec{k}') m_{ij}^{(\alpha)}(\hat{\vec{k}}) m^{(\beta)ij}(\hat{\vec{k}'}) (2\pi)^3 \delta(\vec{k} + \vec{k}') \\ &= \frac{1}{2} \sum_{\alpha=+,\times} \int \mathrm{d}^3\mathrm{k} \, [h'^{(\alpha)}(\eta, \vec{k})]^2, \end{aligned}$$

where the apostrophe in k is used to distinguished between different modes and not to be confused with the apostrophe in $\mathcal{H}_{ij}$ which is its derivative with respect to conformal time, η. Likewise, the second term is given by:

$$\int \partial_i \mathcal{H}_{jk} \partial^i \mathcal{H}^{jk} \, \mathrm{d}^3\mathrm{x} = -\frac{1}{2} \sum_{\alpha=+,\times} \int \mathrm{d}^3\mathrm{k} \, k^2 [h^{(\alpha)}(\eta, \vec{k})]^2.$$

Thus, the second-order tensor perturbation action is simplified as:

$$\mathcal{S}^{(2)} = \frac{M_{Pl}^2}{16} \sum_{\alpha=+,\times} \int a^2 [\{h'^{(\alpha)}\}^2 + k^2 \{h^{(\alpha)}\}^2] \, \mathrm{d}\eta \mathrm{d}^3\mathrm{x}. \tag{4.24}$$

By inspecting this action and its similarities to the second-order inflation action, (4.3), we can quantise it following the method laid out in subsubsection 4.1.2 using the redefinition $\delta\varphi = \frac{M_{Pl}}{\sqrt{8}} h^{(\alpha)}$ [69].

Finally, its power spectrum is inferred from the tensor-perturbation quantum variance,

$$\langle h^{(\alpha)}(\vec{k})[h^{(\alpha)}(\vec{k'})]^*\rangle \equiv \frac{2\pi^2}{k^3}\mathcal{P}_h(k)\delta(\vec{k}-\vec{k'}). \tag{4.25}$$

At horizon crossing ($k\eta = 1$), the power spectrum takes the form [69]:

$$\mathcal{P}_h(k) = \frac{8}{M_{Pl}^2}\left(\frac{H_k}{2\pi}\right)^2. \tag{4.26}$$

The *tensor spectral index*, n_t which serves a similar purpose to its scalar counterpart, is defined as:

$$n_t = \frac{\mathrm{d}\ln\mathcal{P}_h(k)}{\mathrm{d}\ln \mathrm{k}}. \tag{4.27}$$

From this, we can formulate an approximate power law for the power spectrum of the tensor perturbation, analogous to (4.18):

$$\mathcal{P}_h(k) = A_t(k_*)\left(\frac{k}{k_*}\right)^{n_t}. \tag{4.28}$$

4.1.6 The Consistency Condition

Now that we have the scalar and tensor power spectra as well as their corresponding spectral indices and approximate power laws, we can use them to determine the *consistency condition* for the single-field slow-roll inflation [69].

We start by defining the *tensor-to-scalar ratio* as

$$r = \frac{A_t}{A_s} = 16\epsilon, \tag{4.29}$$

using equations (4.16), (4.26), (4.18) and (4.28). However, if we recall the tensor spectral index in equation (4.27) and substitute in the slow-roll parameters (1.23), (1.24) as well as the tensor perturbation power spectrum, (4.26) we will find that

$$\begin{aligned} n_t &= \frac{\mathrm{d}\ln\mathcal{P}_h}{\mathrm{d}\ln \mathrm{a}}\frac{\mathrm{d}\ln \mathrm{a}}{\mathrm{d}\ln \mathrm{k}} \\ &= 2\frac{\mathrm{d}\ln \mathrm{H}}{\mathrm{d}\ln \mathrm{a}}\left(\frac{\mathrm{d}\ln \mathrm{k}}{\mathrm{d}\ln \mathrm{a}}\right)^{-1}\Bigg|_{k=aH} \\ &= -2\epsilon(1-\epsilon)^{-1} \\ &\approx -2\epsilon, \end{aligned}$$

where $\frac{\mathrm{d}\ln \mathrm{k}}{\mathrm{d}\ln \mathrm{a}} = 1-\epsilon$ comes from the fact that $\ln \mathrm{k} = \ln \mathrm{a} + \ln \mathrm{H}$ at horizon crossing [69]. Thus, by substituting this result into equation (4.29), we conclude the consistency condition to be:

$$r \approx -8n_t. \tag{4.30}$$

4.1.7 Computational Methods

We spent the preceding subsubsections deriving the primordial perturbation power spectra and their related quantities analytically, however one could perform these calculations numerically as well. The computational method involves solving highly oscillatory ordinary differential equations (ODEs) whose details are beyond the scope of this dissertation. For interested readers, some literature relevant to this topic include [4, 5, 34, 71].

4.2 Important Results

Here, we summarise the important quantities derived in subsection 4.1.

Power Spectrum of Inflation

$$\mathcal{P}_{\delta\varphi}(k) = \left(\frac{H}{2\pi}\right)^2 \Bigg|_{k=aH} \equiv \left(\frac{H_k}{2\pi}\right)^2$$

Power Spectrum of Curvature Perturbation

$$\mathcal{P}_{\mathfrak{R}}(k) = \frac{1}{2M_{Pl}^2\epsilon}\left(\frac{k}{2\pi a}\right)^2$$

Scalar Spectral Index

$$n_s = 1 + \frac{\mathrm{d}\ln\mathcal{P}_{\mathfrak{R}}(k)}{\mathrm{d}\ln \mathrm{k}}$$

Power-Law Approximation of Curvature Perturbation

$$\mathcal{P}_{\mathfrak{R}}(k) = A_s(k_*)\left(\frac{k}{k_*}\right)^{n_s-1}$$

Power Spectrum of Tensor Perturbation

$$\mathcal{P}_h(k) = \frac{8}{M_{Pl}^2}\left(\frac{H_k}{2\pi}\right)^2$$

Tensor Spectral Index

$$n_t = \frac{\mathrm{d}\ln\mathcal{P}_h(k)}{\mathrm{d}\ln \mathrm{k}}$$

Power-Law Approximation of Tensor Perturbation

$$\mathcal{P}_h(k) = A_t(k_*)\left(\frac{k}{k_*}\right)^{n_t}$$

Tensor-to-Scalar Ratio

$$r = \frac{A_t}{A_s} = 16\epsilon$$

Consistency Condition for a Single-Field Slow-Roll Inflation

$$r \approx -8n_t$$

4.3 Significance of Power Spectra Quantities

The quantities derived in subsection 4.2 are crucial in our understanding of primordial perturbations as they act as a bridge between theory and observation. Thus, in this subsection, we will highlight their significance in observation and their ability to unveil the mysteries of inflation.

Firstly, the power spectrum is a crucial parameter which discerns the contribution of perturbation modes to the total variance. Hence, one of the goals of observation is to determine the shape of the primordial spectra, as these set the initial conditions of inflation [51]. For such a task, the approximate power-laws are preferred. In these power laws, the primordial perturbation power spectra are characterised by the scalar spectral index, n_s:

$$\begin{aligned} n_s < 1 &: \text{red} - \text{tilted}, \\ n_s = 1 &: \text{scale} - \text{invariant}, \\ n_s > 1 &: \text{blue} - \text{tilted}. \end{aligned}$$

The scale-invariant spectrum is also known as the Harrison-Zel'dovich-Peebles spectrum. Any deviations from this is either indicated by the red and blue tilts or by the running of the scalar spectral index [69],

$$\alpha_s = \frac{\mathrm{d}n_s}{\mathrm{d}\ln \mathrm{k}}. \tag{4.31}$$

The indices are measured on scales probed by the CMB. According to the slow-roll approximation model, α_s has typically low values as it contains second-order slow-roll parameters [18]. A $\alpha_s = 0$ detection by instruments incapable of reaching second-order levels of sensitivity agrees with this prediction, however it is worth noting its negative mean values [18]. As for the scalar spectral index, observations favour a slightly red-tilted spectrum, which points to a negative curvature of the potential, $V_{,\varphi\varphi} < 0$ [69]. Similarly, a single-field slow-roll model predicts a red tilt in the tensor spectral index, n_t, though some scenarios may benefit from a blue-tilt measurement of this quantity. Unlike the scalar modes, the tensor modes have yet to be detected.

It is worth noting that in 2003, a study was done on the possibility of a *running scalar spectral index*[35], a case in which the scalar spectral index value varies with the scale on which it is measured[36] [21]. Motivated by the Wilkinson Microwave Anisotropy Probe (WMAP) data at the time [16], the study predicted a blue-tilted spectrum at small k and a red-tilted spectrum at large k. Despite the interesting premise of this study, the notion of a running scalar spectral index provided some challenges:

1. It dictates a large third field derivative whilst maintaining the current small first and second field derivatives in most slow-roll models.

2. Its related calculations result in a shorter period of inflation, thus the 60 e-folds are not sustained.

3. It requires a locally-flat region of the inflation potential, $V(\varphi)$.

As the paper concludes, several adjustments would have to be made for this running scalar spectral index to fit with our current understanding of inflation. This depicts the importance of the power spectra and spectral indices in determining the most reliable models of inflation.

[35] Not to be confused with the running *of* the scalar spectral index, α_s previously introduced.

[36] Long-length scales correspond to small k-values whereas short-length scales correspond to large k-values.

Additionally, the consistency condition helps to rule out inflationary models that are not compatible with observational data. In [69], the single-field slow roll, generic single-field and multi-field inflationary models are discussed, with their respective consistency conditions summarised in the table[37] below.

Table 1: Consistency conditions of different inflationary models.

Inflationary Model	Consistency Condition
Single-field slow-roll	$r = -8n_t$
Generic single-field	$r = -8n_t c_s$
Multifield	$r = -8n_t \sin^2 \Lambda$

In Table 1, c_s is the speed of sound and $\sin^2 \Lambda$ characterises the ratio between the power spectrum as they leave the horizon during inflation and the observed power spectrum [69]. By inspection, a common factor among the different consistency conditions is the tensor spectral index, n_t. Hence, PGW-detection is paramount to our understanding of inflation. In fact, the detected tensor spectral index relates to the inflationary model constraints via [69]:

$$\begin{aligned} n_s - 1 &= 2\tau_V - 6\epsilon_V, \\ n_t &= -2\epsilon_V. \end{aligned} \tag{4.32}$$

Ultimately, the primordial perturbation power spectra, scalar and tensor spectral indices as well as the consistency condition are important parameters in decoding inflation. These quantities constrain the initial conditions of inflation and control the shape of the potential, $V(\varphi)$, thus they act as a bridge between theory and observation. One could apply a particular ansatz of the scalar spectral index such as the Harrison-Zel'dovich-Peebles spectrum to predict prospective observables, or compare observational data to existing inflationary models to pinpoint the one which is most consistent with the chronology of epochs that took place during the early age of the universe. In the following section, we shall summarise some interesting development on PGW-detection.

[37] This table was reproduced from [69].

5 Discussion: Primordial Gravitational-Wave Detection

This section provides a brief, qualitative discussion of effort in detecting PGWs, that starts with the motivation behind this field of research (which is essentially an expansion of subsubsection 1.1.2), followed by some description of PGW-detection works via the CMB and stochastic GW-backgrounds.

5.1 Motivations for Detection

There are many motivations behind cosmologists' search for PGWs. These include:

1. **Establishing the theory of inflation as a standard model of cosmology**. Despite the theory's successes in solving puzzles related to the hot Big Bang model as elaborated in subsubsection 1.2.2 and subsection 2.1, it lacks solid proof. Moreover, compared to its rival theories, inflation is the only one that successfully explains a smooth transition into the Big Bang model and predicts the existence of PGWs [69]. Thus, discovery of these PGWs is crucial in granting its legitimacy as a concrete cosmological model.

2. **Filtering and testing inflationary models**. While this dissertation solely focuses on the slow-roll approximation model of inflation, various alternative models exist. Therefore, detecting the amplitudes and spectral index of PGWs puts constraints on inflationary models and determines any violation of the consistency condition, which will in turn narrow down the inflationary model most accurate with our observed universe.

3. **Extracting information about the early universe and making better predictions**. Data obtained from measured PGWs could be extrapolated to determine the energy scale as well as initial conditions of inflation and thus, that of the early universe. To date, the energy scales and initial conditions used in inflationary models have been mere estimates, hence such models could further benefit from improvements made using their actual values. In fact, these newly-enhanced models would also better predict observables of the theory, thus improving observational methods and instruments.

4. **Understanding the physics behind inflation and beyond the standard model**. There is much speculation regarding the fundamental theories behind inflation including string theory, which is closely linked to quantum gravity and supersymmetry [69]. Thus, PGW-detection along with any information about inflation obtained from it may hint at how these fundamental theories could add on to the standard model of particle physics.

5.2 PGW Traces in the CMB

The CMB radiation observed today is essentially a snapshot of photons that last scattered off electrons at the time of recombination, thus contains information on various properties of the primordial universe [18]. The radiation possesses a blackbody spectrum with a temperature of approximately 2.728K [50]. Its properties were first predicted by Alpher and Hermann in their works in 1948 and 1949 [8, 9] but only discovered in 1965 by Penzias and Wilson [52, 53], who stumbled upon the radiation whilst looking for neutral hydrogen. 27 years later, anisotropies in the radiation were finally detected by the Cosmic Background Explorer (COBE) Differential Microwave Radiometers (DMR) [69] following scepticism regarding its homogeneity and isotropy. The suggested link between these anisotropies and primordial perturbations generated during inflation has motivated cosmologists to study them for clues of inflation, particularly PGWs. There are two intrinsic properties to take note when observing the CMB - *temperature anisotropy* and *polarisation*.

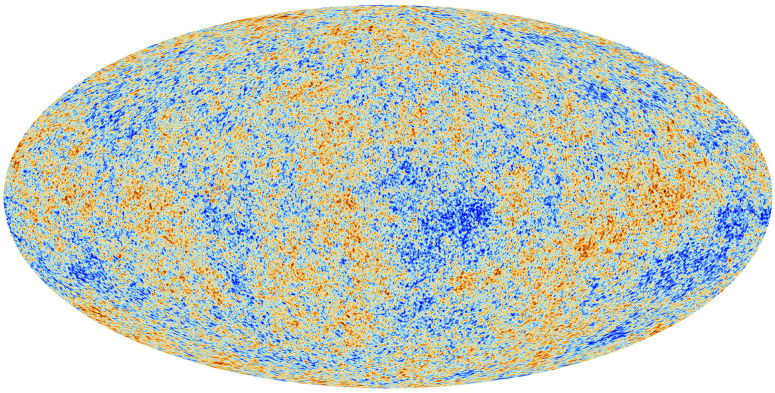

Figure 4: Anisotropies of the CMB in the form of temperature fluctuations which correspond to patches of different densities captured by Planck. Credit: ESA and the Planck Collaboration.

5.2.1 Temperature Anisotropy

Both scalar and tensor perturbations contribute to the temperature anisotropy of the CMB, however only the scalar modes have been detected thus far. There are two types of spectral distortions in the CMB: μ- and y-types. In 2014, a study demonstrated the use of Silk damping effects to distinguish between μ distortions produced by scalar perturbations and tensor perturbations [48]. In relation to this, a new mechanism of μ-type distortion generated by tensor perturbations was proposed and compared to the established mechanism for scalar perturbations. The results show that while μ distortions from scalar perturbations were mostly created at the Silk damping scale, tensor perturbations produce these distortions through Thomson scattering, which occurs at much larger scales than Silk damping [48]. By restricting the tensor-to-scalar ratio and the tensor spectral index, n_t to scale-invariance, the μ distortion coming from PGWs was found to be very tiny ($\approx 10^{-13}$). In fact, the value would only be significant for a blue-tilted n_t [48]. Regardless, by identifying the sources of μ distortion through their scale-dependence, one could obtain indirect evidence for PGWs.

5.2.2 B-Mode Polarisation

The polarisation of the CMB is split into E-modes and B-modes. Since scalar perturbations produce the former whereas tensor perturbations produce both, the B-mode polarisation is preferred when searching for PGWs in the CMB. It is worthy to note that PGWs are not the sole contributor to B-mode polarisation in the CMB. In fact, other phenomena that could result in the polarisation include topological effects, global phase transition, primordial inhomogeneities magnetic fields and gravitational lensing [69]. Nonetheless, these barely hinder PGW-detection as they are either trivial compared to the PGW contribution, or easily distinguishable due to their non-Gaussinity properties and presence of the Faraday effect [69]. The major obstacle in detecting the B-modes is their small magnitude which are one order of magnitude smaller than that of E-modes [69] and made weaker in the presence of astrophysical foreground. In fact, the only significant detection of B-mode polarisation - which was done by a CMB polarimeter from the BICEP2 experiment in the South Pole [3] - was revealed to be emitted from dust in the Milky Way after cross analysis with data recorded by the Planck satellite [2]. Thus, to move forward in B-mode polarisation detection, it is crucial to improve sensitivity of existing detectors and develop better techniques to filter the foreground signals. For example, [54] introduces a new metamaterial that could potentially improve such detections as it operates over a wide microwave frequency range.

5.3 PGW-Extraction from Stochastic GWs

While the CMB radiation is arguably the best probe we have of the early universe, it did not deter researchers from investigating alternative methods. One such alternative is to extract PGW-signals from a background of directly-detected *stochastic GWs*. Stochastic GWs refers to a superposition of gravitational waves from independent sources coming from all directions [20]. A GW-analogue of the CMB, they appear as noise on a GW-detector [20]. Thus, to extract any PGW-signal, the detected background must be cross-analysed between different detectors.

In 1999, Polarski tested the possibility of this method in the framework of a Lambda-Cold Dark Matter (ΛCDM) broken-scale-invariant (BSI) models. He found that, with the BSI models, the instrumental sensitivity required to measure PGWs is one magnitude lower than the initial sensitivity needed for single-field slow-roll models [57]. In fact, for a BSI inflation model that matches observation in particular, there would be less constraints on PGW detection should the slow-roll approximation be more lenient [57]. However, despite his rather positive findings, Polarski was doubtful these sensitivities would be reached in the near future. Seven years later, numerical work was published on the prospects of directly-detecting PGWs for single-field inflationary models.

Motivated by the fact that prior studies on stochastic GW-background were always reliant on the form of inflationary potential (as energy scales of inflation are unknown), the pair of authors sought to make more generic predictions with regards to PGW-detection [19]. The paper concluded a rather pessimistic outlook on direct-detection of PGWs from slow-roll inflation models, however offered compensation by listing down other possible cosmological sources that would produce PGWs available in the frequency range of current and upcoming direct-detection experiments such as Advanced LIGO, the Laser Interferometer Space Antenna (LISA), NASA's Big Bang Observer (BBO), Japan's DECi-hertz Interferometer Gravitational Wave Observatory (DECIGO) and Ultimate DECIGO [19]. Apart from this paper, in [20], Christensen also elaborates on the different cosmological and astrophysical sources of GWs one could find in a stochastic background, including PGWs produced during inflation, as well as the methods to constrain them. While his evaluation was strictly focused on Advanced LIGO and Advanced Virgo, the author hoped that the upcoming launch of LISA will bring tremendous insight into stochastic GW-backgrounds [20].

Two years after the publication of Christensen's paper, a team of researches from the US and Australia had published a paper in which they pointed out one major flaw of extracting PGW signals from a stochastic GW background - there would be astrophysical GW-foreground coming from far-away mergers whose signals are just as faint as those predicted to come from PGWs [17]. Such signals would be hard to distinguish from PGW-signals, thus jeopardising the accuracy of data. This piece of information seem to be overlooked by most literature discussing stochastic GW-detection. The team proposed an alternate method - rather than relying on established constraints, they emphasised on simulating GW-pattern from astrophysical mergers [17]. They believe that familiarity with the patterns would allow for more accurate classification of every astrophysical signal present in the stochastic GW-background, and thus better removal of these signals to find the PGW pattern.

In the paper, they recall analysing 404s seconds of simulated astrophysical GW-pattern injected with a faint signal analogous to the 'persistent hum' of PGWs [17]. In their application of the method, they had to analyse the data over various simulation runs with different sets of initial conditions. Eventually, they were able to successfully extract the simulated PGW signals. The fact that PGWs maintain a similar pattern on any two detectors in contrast to astrophysical GWs which behave uniquely to the detector [17] means that cross-analysis between data from different detectors would ease the extraction process tremendously. It is their hope that the methods established in this paper would be adopted once currently-proposed GW detectors go online. In fact, they ambition that initial conditions of the early universe may also be determined, by comparison with the initial conditions required for the simulation to produce similar PGW patterns. This is by far one of the most innovative work I have encountered on stochastic GW-detection.

Despite the flaw related to extracting PGW signals from stochastic GW backgrounds mentioned in the above paper, perhaps it was too early to rule out possible improvements. Early this year, the detection prospects of stochastic GWs using the upcoming LISA were summarised [28]. The study had found a key feature that would differentiate between stochastic GW-background created during inflation and those created after inflation. The secret lies in the frequency profile of the signal - oscillations from the former appear on the ultraviolet (UV) tail of its spectrum whereas the latter's oscillations modulate the peak of its GW spectrum [28]. This means that GWs produced after inflation would peak at different frequencies while PGWs would generally have much higher peaks. This would allow accurate extraction of PGW signals despite their amplitude having the same magnitude as other astrophysical mergers. The results of this paper have proven that at small scales, one could target the frequency profiles of stochastic GWs to determine the legitimacy of the inflation theory [28].

With the upcoming launch of many GW detectors in place for the next decade, it will be interesting to see if such PGW-detection prospects are realised.

6 Conclusion

Our standard model of cosmology is incomplete without addressing the problems arising from inconsistencies between the established hot Big Bang model and observational data. While the hot Big Bang model successfully describes the mechanisms by which our universe expands and its matter content is produced, it fails to explain why the universe is homogeneous at large scales and how small density fluctuations could have existed to form the galaxy clusters and stars we observe today. Thus, additional mechanisms are required to solve these anomalies whilst still maintaining the successes of the hot Big Bang model. The theory of inflation is a leading candidate in this race as its premises simultaneously solve both problems, as well as the flatness problem and the monopole problem, which were not covered in this dissertation. By introducing an epoch of a rapid, accelerated expansion which took place before the radiation-dominated epoch, the theory proposed that the 'causally-disconnected' regions of the universe had achieved uniform temperature back when they were within one small, causal patch. Likewise, the large-scale structure of the universe was thought to have formed from vacuum quantum fluctuations which were later stretched to cosmic scales due to inflation.

To account for these fluctuations, linear perturbations were added to the metric in terms of scalar functions, Ψ and Φ and the divergenceless, traceless and symmetric tensor $\mathcal{H}_{ij}$. Using this perturbed metric to derive the perturbed Einstein equations, we arrived at a set of evolution equations for the scalar perturbations and the tensor perturbations. The former illustrates dynamics that depends on the matter distribution of the universe, hence indicating that scalar perturbations directly contribute to the formation of the large-scale structure. The latter, on the other hand, takes the form of a wave equation with no source, thus implying that inflation predicts the existence of PGWs. By quantising the perturbations, their power-spectra power laws and spectral indices were formulated. These, along with the consistency condition of a particular inflationary model[38], are used to constrain the initial conditions and shape of the potential of inflation, $V(\varphi)$. Such constraints are hoped to distinguish inflationary models that best describe our universe. To achieve this, PGW-detection is essential. In the wake of a direct GW-detection by LIGO, much research has been done to develop better computational methods and detectors specialised for PGW-detection.

To put the timeline into perspective, the theory of inflation was first published in 1981, and within the first few years of its formation, the mathematics behind its primordial perturbations were also formulated, including the prediction of PGWs. While methods to detect PGWs to prove the legitimacy of the theory were developed as early as in the 90's, it is only in the 21$^{\text{st}}$ century that we are able to see these plans unfold[39]. If there is one takeaway from this, it is that our ideas and exploration of the universe around us are only limited by the technological limitations of our time. While it is a shame to know that we may not live to witness future generations materialising our own theoretical predictions[40], as scientists, we shall do our best with the tools that we have, to honour the theories that came before us. With recent advancements in technological instruments as well as artificial intelligence (AI) and machine learning (ML) algorithms, it is undoubtedly an exciting time to be working on GW and PGW-detection, and just in science, generally.

[38] In this dissertation, we focused on the single-field slow-roll approximation model.

[39] The same can be said about GWs from astrophysical mergers that were predicted in Einstein's theory of general relativity.

[40] Much like Einstein never got to experience the Advanced LIGO detection.

References

[1] B. P. Abbott, R. Abbott, T. D. Abbott, M. R. Abernathy, F. Acernese, K. Ackley, C. Adams, T. Adams, P. Addesso, R. X. Adhikari, et al. Observation of gravitational waves from a binary black hole merger. *Phys. Rev. Lett.*, 116:061102, Feb 2016.

[2] P. A. R. Ade, N. Aghanim, Z. Ahmed, R. W. Aikin, K. D. Alexander, M. Arnaud, J. Aumont, C. Baccigalupi, A. J. Banday, D. Barkats, R. B. Barreiro, J. G. Bartlett, N. Bartolo, E. Battaner, K. Benabed, A. Benoît, A. Benoit-Lévy, S. J. Benton, J.-P. Bernard, et al. Joint analysis of bicep2/keck array and planck data. *Phys. Rev. Lett.*, 114:101301, Mar 2015.

[3] P. A. R. Ade, R. W. Aikin, D. Barkats, S. J. Benton, C. A. Bischoff, J. J. Bock, J. A. Brevik, I. Buder, E. Bullock, C. D. Dowell, L. Duband, J. P. Filippini, S. Fliescher, S. R. Golwala, M. Halpern, M. Hasselfield, S. R. Hildebrandt, G. C. Hilton, V. V. Hristov, K. D. Irwin, K. S. Karkare, J. P. Kaufman, B. G. Keating, S. A. Kernasovskiy, J. M. Kovac, C. L. Kuo, E. M. Leitch, M. Lueker, P. Mason, C. B. Netterfield, H. T. Nguyen, R. O'Brient, R. W. Ogburn, A. Orlando, C. Pryke, C. D. Reintsema, S. Richter, R. Schwarz, C. D. Sheehy, Z. K. Staniszewski, R. V. Sudiwala, G. P. Teply, J. E. Tolan, A. D. Turner, A. G. Vieregg, C. L. Wong, and K. W. Yoon. Detection of b-mode polarization at degree angular scales by bicep2. *Phys. Rev. Lett.*, 112:241101, Jun 2014.

[4] F. Agocs and A. Lasenby. *Primordial evolution of cosmological perturbations: Theory and computation.* PhD thesis, 2021.

[5] F. J. Agocs, W. J. Handley, A. N. Lasenby, and M. P. Hobson. Efficient method for solving highly oscillatory ordinary differential equations with applications to physical systems. *Phys. Rev. Res.*, 2(1):013030, 2020.

[6] K. Akiyama, A. Alberdi, W. Alef, K. Asada, R. Azulay, A.-K. Baczko, D. Ball, M. Balokovic, J. Barrett, D. Bintley, and others. First m87 event horizon telescope results. iv. imaging the central supermassive black hole. *The Astrophysical Journal*, 875(1), Apr 2019.

[7] A. Albrecht, P. J. Steinhardt, M. S. Turner, and F. Wilczek. Reheating an inflationary universe. *Physical Review Letters*, 48(20):1437–1440, May 1982.

[8] R. A. ALPHER and R. HERMAN. Evolution of the universe. *Nature*, 162(4124):774â775, Nov 1948.

[9] R. A. Alpher and R. C. Herman. Remarks on the evolution of the expanding universe. *Phys. Rev.*, 75:1089–1095, Apr 1949.

[10] C. Antolini, M. Martinelli, Y. Fantaye, and C. Baccigalupi. Measuring primordial gravitational waves from CMBib/i-modes in cosmologies with generalized expansion histories. *Journal of Cosmology and Astroparticle Physics*, 2013(02):024–024, feb 2013.

[11] M. Artymowski, O. Czerwińska, Z. Lalak, and M. Lewicki. Gravitational wave signals and cosmological consequences of gravitational reheating. *Journal of Cosmology and Astroparticle Physics*, 2018(04):046–046, apr 2018.

[12] A. J. Banday and A. W. Wolfendale. Fluctuations in the cosmic microwave background. , 245:182, July 1990.

[13] J. M. Bardeen, P. J. Steinhardt, and M. S. Turner. Spontaneous creation of almost scale-free density perturbations in an inflationary universe. *Phys. Rev. D*, 28:679–693, Aug 1983.

[14] D. Baumann. Tasi lectures on inflation, 2009.

[15] C. Bennett, A. Banday, K. Gorski, G. Hinshaw, P. Jackson, P. Keegstra, A. Kogut, G. Smoot, D. Wilkinson, and E. Wright. Four-year cobe dmr cosmic microwave background observations: Maps and basic results. *Astrophysical Journal - ASTROPHYS J*, 464, 06 1996.

[16] C. L. Bennett, M. Halpern, G. Hinshaw, N. Jarosik, A. Kogut, M. Limon, S. S. Meyer, L. Page, D. N. Spergel, G. S. Tucker, E. Wollack, E. L. Wright, C. Barnes, M. R. Greason, R. S. Hill, E. Komatsu, M. R. Nolta, N. Odegard, H. V. Peiris, L. Verde, and J. L. Weiland. First-year wilkinson microwave anisotropy probe (wmap) observations: Preliminary maps and basic results. *The Astrophysical Journal Supplement Series*, 148(1):1–27, sep 2003.

[17] S. Biscoveanu, C. Talbot, E. Thrane, and R. Smith. Measuring the primordial gravitational-wave background in the presence of astrophysical foregrounds. *Phys. Rev. Lett.*, 125:241101, Dec 2020.

[18] A. Challinor and H. Peiris. Lecture notes on the physics of cosmic microwave background anisotropies. *AIP Conference Proceedings*, 1132(1):86–140, 2009.

[19] S. Chongchitnan and G. Efstathiou. Prospects for direct detection of primordial gravitational waves. *Phys. Rev. D*, 73:083511, Apr 2006.

[20] N. Christensen. Stochastic gravitational wave backgrounds. *Reports on Progress in Physics*, 82(1):016903, nov 2018.

[21] D. J. H. Chung, G. Shiu, and M. Trodden. Running of the scalar spectral index from inflationary models. *Phys. Rev. D*, 68:063501, Sep 2003.

[22] P. Coles. Einstein, eddington and the 1919 eclipse, Apr 2019.

[23] S. Dodelson. *Modern Cosmology*. Academic Press, 2003.

[24] F. W. Dyson, A. S. Eddington, and C. Davidson. Ix. a determination of the deflection of light by the sun's gravitational field, from observations made at the total eclipse of may 29, 1919. *Philosophical Transactions of the Royal Society of London. Series A, Containing Papers of a Mathematical or Physical Character*, 220(571-581):291–333, Jan 1920.

[25] G. F. R. Ellis. Editorial note to: E. lifshitz, on the gravitational stability of the expanding universe. *General Relativity and Gravitation*, 49(2), Jan 2017.

[26] D. Falk. One hundred years ago, einstein's theory of general relativity baffled the press and the public, Nov 2019.

[27] A. Friedmann. On the curvature of space. *General Relativity and Gravitation*, 31(12):1991–2000, 1999.

[28] J. Fumagalli, M. Pieroni, S. Renaux-Petel, and L. T. Witkowski. Detecting primordial features with LISA. *Journal of Cosmology and Astroparticle Physics*, 2022(07):020, jul 2022.

[29] J. Garcia-Bellido. Primordial gravitational waves and the local b-mode polarization of the cmb. 05 2010.

[30] A. H. Guth. Inflationary universe: A possible solution to the horizon and flatness problems. *Physical Review D*, 23(2):347–356, Jan 1981.

[31] A. H. Guth and S.-Y. Pi. Fluctuations in the new inflationary universe. *Phys. Rev. Lett.*, 49:1110–1113, Oct 1982.

[32] A. H. Guth and S.-Y. Pi. Quantum mechanics of the scalar field in the new inflationary universe. *Phys. Rev. D*, 32:1899–1920, Oct 1985.

[33] A. H. Guth and E. J. Weinberg. Could the universe have recovered from a slow first-order phase transition? *Nuclear Physics B*, 212(2):321–364, 1983.

[34] W. Haddadin and W. Handley. Rapid numerical solutions for the mukhanov-sasaki equation. *Physical Review D*, 103, 06 2021.

[35] S. W. Hawking, I. G. Moss, and J. M. Stewart. Bubble collisions in the very early universe. *Phys. Rev. D*, 26:2681–2693, Nov 1982.

[36] S. Hossenfelder. Is the inflationary universe a scientific theory? not anymore, Sep 2017.

[37] E. Hubble. A relation between distance and radial velocity among extra-galactic nebulae. *Proceedings of the National Academy of Sciences*, 15(3):168–173, Apr 1929.

[38] M. Kamionkowski and E. D. Kovetz. The quest for b modes from inflationary gravitational waves. *Annual Review of Astronomy and Astrophysics*, 54(1):227–269, 2016.

[39] A. V. Kravtsov and S. Borgani. Formation of galaxy clusters. *Annual Review of Astronomy and Astrophysics*, 50(1):353–409, 2012.

[40] E. Landau. A total solar eclipse 100 years ago proved einstein's general relativity, May 2019.

[41] G. Lemaître. Republication of: A homogeneous universe of constant mass and increasing radius accounting for the radial velocity of extra-galactic nebulae. *General Relativity and Gravitation*, 45(8):1635–1646, Jun 2013.

[42] N. Lemarchand. *Impacts of cosmic inhomogeneities on the CMB : primordial perturbations in two-field bouncing cosmologies and cosmic magnetism in late-time structures*. Theses, Université Paris Saclay (COmUE), Dec. 2019.

[43] A. R. Liddle and D. H. Lyth. *Cosmological Inflation and Large-Scale Structure*. Cambridge University Press, 2000.

[44] A. D. Linde. A new inflationary universe scenario: A possible solution of the horizon, flatness, homogeneity, isotropy and primordial monopole problems. *Physics Letters*, 108B(6):389–393, Feb 1982.

[45] J. Maldacena. Non-gaussian features of primordial fluctuations in single field inflationary models. *Journal of High Energy Physics*, 2003(05):013–013, may 2003.

[46] I. Moss. *The Quantum Origin of the Universe*, pages 1–18. Springer Netherlands, Dordrecht, 1988.

[47] V. Mukhanov. *Physical Foundations of Cosmology*. Cambridge University Press, 2005.

[48] A. Ota, T. Takahashi, H. Tashiro, and M. Yamaguchi. CMB distortion from primordial gravitational waves. *Journal of Cosmology and Astroparticle Physics*, 2014(10):029–029, oct 2014.

[49] D. Overbye. A famous black hole gets a massive update, Feb 2021.

[50] L. Page and D. Wilkinson. *Cosmic Microwave Background Radiation*, pages 291–301. Springer New York, New York, NY, 1999.

[51] Paykari, P., Lanusse, F., Starck, J.-L., Sureau, F., and Bobin, J. Prism: Sparse recovery of the primordial power spectrum. *A&A*, 566:A77, Jun 2014.

[52] P. J. E. Peebles. Penzias & Wilson's Discovery of the Cosmic Microwave Background. , 525C:1067, Nov. 1999.

[53] A. A. Penzias and R. W. Wilson. A Measurement of Excess Antenna Temperature at 4080 Mc/s. , 142:419–421, July 1965.

[54] G. Pisano, B. Maffei, P. A. R. Ade, P. de Bernardis, P. de Maagt, B. Ellison, M. Henry, M. W. Ng, B. Schortt, and C. Tucker. Multi-octave metamaterial reflective half-wave plate for millimeter and sub-millimeter wave applications. *Appl. Opt.*, 55(36):10255–10262, Dec 2016.

[55] Planck Collaboration, Ade, P. A. R., Aghanim, N., Arnaud, M., Arroja, F., Ashdown, M., Aumont, J., Baccigalupi, C., Ballardini, M., Banday, A. J., Barreiro, R. B., et al. Planck 2015 results - xvii. constraints on primordial non-gaussianity. *A&A*, 594:A17, 2016.

[56] Planck Collaboration, Akrami, Y., Arroja, F., Ashdown, M., Aumont, J., Baccigalupi, C., Ballardini, M., Banday, A. J., Barreiro, R. B., Bartolo, N., et al. Planck 2018 results - x. constraints on inflation. *A&A*, 641:A10, 2020.

[57] D. Polarski. Direct detection of primordial gravitational waves in a bsi inflationary model. *Physics Letters B*, 458(1):13–18, 1999.

[58] R. N. R. *A Study of Inflationary Paradigm*. PhD thesis, 2014.

[59] A. G. Riess, A. V. Filippenko, P. Challis, A. Clocchiatti, A. Diercks, P. M. Garnavich, R. L. Gilliland, C. J. Hogan, S. Jha, R. P. Kirshner, B. Leibundgut, M. M. Phillips, D. Reiss, B. P. Schmidt, R. A. Schommer, R. C. Smith, J. Spyromilio, C. Stubbs, N. B. Suntzeff, and J. Tonry. Observational evidence from supernovae for an accelerating universe and a cosmological constant. *The Astronomical Journal*, 116(3):1009–1038, sep 1998.

[60] A. Riotto. Inflation and the theory of cosmological perturbations, 2002.

[61] J. A. Romeu. Derivation of friedman equations, Jun 2014.

[62] B. Schwarzschild. High-redshift supernovae indicate that dark energy has been around for 10 billion years. *Physics Today*, 60(1):21–25, 2007.

[63] A. K. Singal. Horizon, homogeneity and flatness problems – do their resolutions really depend upon inflation?, 2016.

[64] A. Starobinsky. Dynamics of phase transition in the new inflationary universe scenario and generation of perturbations. *Physics Letters B*, 117(3):175–178, 1982.

[65] C. Strege and C. R. Contaldi. A comparison of two cosmological models: Inflationary cosmology and the cyclic universe. 2010.

[66] L. A. Ureña-López. Scalar fields in cosmology: dark matter and inflation. *Journal of Physics: Conference Series*, 761:012076, oct 2016.

[67] J.-P. Uzan. The big-bang theory: construction, evolution and status, 2016.

[68] A. Vankov. Einstein's paper: "explanation of the perihelion motion of mercury from general relativity theory". 20, 01 2011.

[69] M. S. Wang. Primordial gravitational waves from cosmic inflation. 2017.

[70] J. M. Weisberg, J. H. Taylor, and L. A. Fowler. Gravitational waves from an orbiting pulsar. *Scientific American*, 245(4):74–82, Oct 1981.

[71] W. Y. Wong. Cosmological recombination, 2008.

[72] D. Wu, H. Li, S. Ni, Z.-W. Li, and C.-Z. Liu. Detecting primordial gravitational waves: A forecast study on optimizing frequency distribution of next generation ground-based cmb telescope. *The European Physical Journal C*, 80(2), Feb 2020.